6. Identification of nonlinear and hysteretic systems

In structural and seismic reliability assessment, dynamic identification is a powerful tool for increasing the level of knowledge of an historic structure. In Chapter 3 linear identification techniques were discussed and applied to relevant real cases of cultural heritage structures. However, when subject to events such as earthquakes, structures typically exhibit a nonlinear and hysteretic behaviour. At this regard, Chapter 5 has reported a wide gamma of models suitable for describing the nonlinear and hysteretic behaviour of masonry elements and structures. In this sixth chapter, several nonlinear identification algorithms will be reviewed with particular emphasis on the distinction among traditional methods and on-line or instantaneous methods. Similarly to the linear case, the identification of a nonlinear system is an inverse problem, whose solutions are functional laws describing the input-output relationships of the system. Conversely, nonlinear identification is a very complex and challenging matter, and has been seldom applied to full-scale structures.

6.1 Identification of nonlinear and evolving systems

Though a reliable evaluation of structural safety conditions should take into account the nonlinear and evolving (e.g. degrading, hysteretic ...) nature of the dynamic response, the experimental identification of a nonlinear behaviour under dynamic and seismic loading is, to date, an unsolved problem. In this context, instantaneous or possibly on-line identification certainly represents an enhancement of the classical approach to nonlinear analysis and control. For instance, on-line implementations of identification methods, such as those based on the restoring force, may provide checks on the consistency of assumptions about the models.

Performance based design of engineering structures subject to dynamic loads calls for expensive experimental tests, whose outcomes, in terms of strength, ductility and dissipation properties, should be assimilated by nonlinear and/or time-varying models. Within the framework of nonlinear structures, the identification process presupposes the availability of a huge quantity of experimental data, much greater than is necessary in linear identification. In this sense, a classification of possible sources of nonlinearity

might still retain a practical interest in structural identification, even if the word nonlinearity has a tautological character. Noteworthy reviews exist in literature about nonlinear identification: for instance, the textbook by Worden and Tomlinson [1] and several comprehensive state-of-the-art papers: e.g. [2,3].

Traditional identification strategies for nonlinear structures are based on the assumptions of weak nonlinearities and on applying small perturbations to the underlying linearised system (e.g. see the recent linearization technique proposed by Sracic *et al* [4]). Nonetheless, the first nonlinear identification approaches were also called linearization techniques such as those proposed by Caughey [5] with the equivalent linearization or by Kazakov [6] with statistical linearization. The harmonic balance method, in particular, has been the basis for several nonlinear system identification techniques (among others see the recent work by Ozer *et al* [7]). This commonly used approach has proved useful in most applications, particularly for the random vibration analysis of systems where the nonlinear restoring force is hysteretic. However, in experimental applications, the extraction of a linear model requires the knowledge of the functional form of the restoring force (see for instance Hagedorn and Wallaschek [8]).

Methods for identifying nonlinear systems are commonly framed into the parametric and the non-parametric approach, respectively: in the parametric case, an a priori selection of a specific model for the dynamic behaviour of the system is needed and the identification process consists of determining the coefficients for such a model. Clearly enough, traditional linearization techniques are usually parametric. Non parametric methods, by contrast, do not require any assumption of the type and localisation of structural nonlinearities but, generally, the quantities identified cannot be directly correlated to the system equation of motion.

A further classification, more relevant to this thesis, can be made among non-instantaneous and instantaneous methods (see table 6.1). The latter can be further framed into on-line methods and off-line methods. An on-line method allows for an identification of the system during the excitation phase and the system parameters are updated at each instant. On the other hand, off-line methods need more data work, and require that the complete excitation process is ended or they need a considerable time-lag for the identification process to be performed.

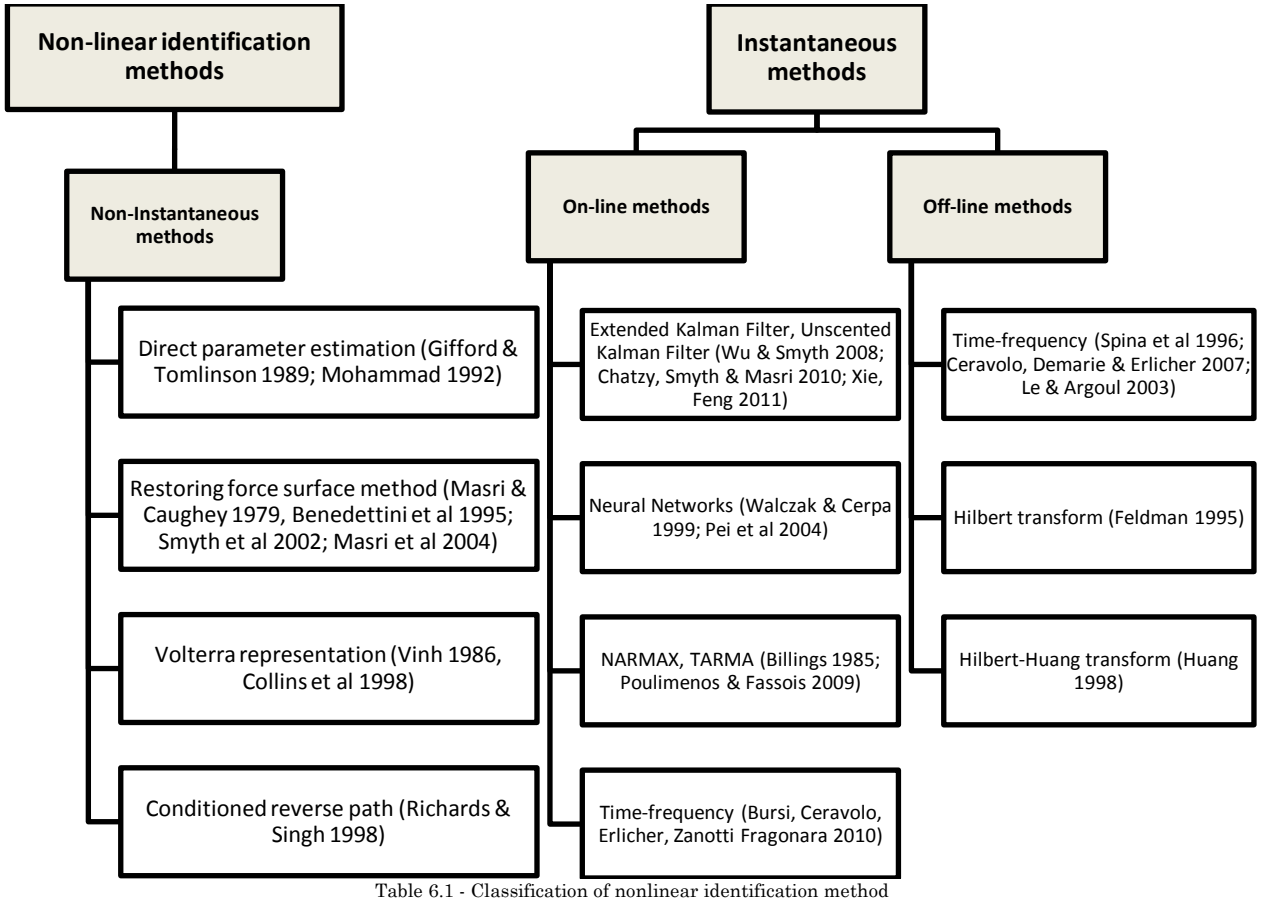

Table 6.1 - Classification of nonlinear identification method

6.2 Models and methods for the identification of nonlinear and evolving systems

6.2.1 Direct Parameter Estimation

The Direct Parameter Estimation (DPE) method is aimed at the identification of the coefficients of the equations of motions for a MDoF system ([1,9,10]).

In MDoF systems the equations of motion are usually assembled by concentrating the mass in *N* points (see figure 6.1): the mass m_i, concentrated in the i^{th} point, interacts with the mass m_j through the force l_{ij} and to the ground by the force l_{ii}. It is assumed that internal forces are dependent only on relative displacements and forces:

$$\begin{cases} l_{ij} = f_{ij}\left(\delta_{ij}, \dot{\delta}_{ij}\right) \\ l_{ii} = f_{ii}\left(\delta_{ii}, \dot{\delta}_{ii}\right) \end{cases} \tag{6.1}$$

with $\delta_{ij} = x_i - x_j$, $\dot{\delta}_{ij} = \dot{x}_i - \dot{x}_j$, $\delta_{ii} = x_i$, $\dot{\delta}_{ii} = \dot{x}_i$.

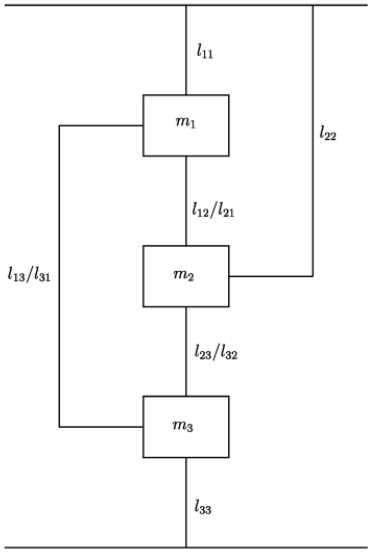

Figure 6.1 - Link model for a 3DoF system.

In common physical systems l_{ij} is equal to l_{ji} therefore the following relation holds:

$$f_{ij}\left(\delta_{ij},\dot{\delta}_{ij}\right)=-f_{ji}\left(\delta_{ji},\dot{\delta}_{ji}\right)=-f_{ji}\left(-\delta_{ij},\dot{\delta}_{ij}\right) \tag{6.2}$$

Equations (6.1) and (6.2) allows for writing the set of nonlinear differential equations which describes the motion of the system:

$$m_i\ddot{x}_i+\sum_{j=1}^{N}f_{ij}\left(\delta_{ij},\dot{\delta}_{ij}\right)=u_i \qquad i=1,...N \tag{6.3}$$

Experimental measures generally consist of the acceleration input to the system and the absolute acceleration of each mass of the system. From the latter, the relative displacements and velocities can be obtained.

A polynomial approximation of the model can be used for f_{ij}:

$$m_i\ddot{x}_i+\sum_{j=1}^{N}\sum_{k=0}^{p}\sum_{l=0}^{q}a_{(ij)kl}\left(\delta_{ij}\right)^k\left(\dot{\delta}_{ij}\right)^l=u_i \qquad i=1,...N \tag{6.4}$$

then, one can use least-square parameter estimation in order to determine which parameters m_i and $a_{(ij)kl}$ best fit the data.

Worden and Tomlinson [1] noticed that an a priori estimation of the masses is not necessary in order to perform an identification, which can be accomplished in two successive steps. In a first step the parameters of the equation of motions which have excitation directly applied are estimated (for instance, DOF 1 in equation (6.5)). Successively, the parameters of the equation with no excitation are identified.

$$\begin{cases} m_1\ddot{x}_1+\sum_{j=1}^{N}\sum_{k=0}^{p}\sum_{l=0}^{q}a_{(1j)kl}\left(\delta_{1j}\right)^k\left(\dot{\delta}_{1j}\right)^l=u_1 \\ \sum_{j=1}^{N}\sum_{k=0}^{p}\sum_{l=0}^{q}a'_{(ij)kl}\left(\delta_{ij}\right)^k\left(\dot{\delta}_{ij}\right)^l=-\ddot{x}_i \qquad i=2,...N \end{cases} \tag{6.5}$$

where $a'_{(ij)kl}=a_{(ij)kl}/m_i$. The coefficients for i=2 can be known up to the scale factor m_2. The coefficients can be determined up to the scale factor m_1 by multiplying both the members of the equation by the ratio m_2/m_1. The procedure can be repeated for all the homogeneous equations recurring to the same scale factor m_1. Once the parameters of the first equation are estimated one can determine the parameters $a'_{(ij)kl}$ and the ratio among masses as follows:

$$\frac{m_i}{m_1}=\frac{a'_{(1i)10}}{a'_{(i1)10}} \tag{6.6}$$

An advantage of this method is that it allows for a natural definition of the restoring force surface for each link. In fact when the model coefficients are identified, forces f_{ij} can be plotted as a function of δ_{ij} and $\dot{\delta}_{ij}$.

6.2.2 Restoring Force Surface method (RFS)

The Restoring Force Surface (RFS) method was originally developed by Masri *et al* [11,12] in order to achieve a non-parametric identification of nonlinear systems. The basic idea behind the method is that the restoring force of a nonlinear system can be expressed in terms of the state variables of the system itself. The method has been also developed autonomously by Crawley and Aubert [13] and by Crawley and O'Donnell [14] through the so-called Force-State Mapping. A further version of the method is present in the literature, as proposed by Duym *et al* [15], and renamed Local RFS.

The motion of an oscillator with nonlinear stiffness is described by Newton's second law in the form:

$$m\ddot{x} + f\left(x,\dot{x}\right) = u\left(t\right) \tag{6.7}$$

where m represents the mass of the system, x the displacement, u the external force, f the internal restoring force of the system. The original RFS method assumes that the restoring force is described by a function of the state variables x and $\dot{x}$: in this way the restoring force can be represented as a surface in the plane $\left(x,\dot{x}\right)$. Once the restoring force surface is defined, it is possible to set the parameters of an analytical model in terms of x and $\dot{x}$ using a least square approximation. Masri at first [11] used a Chebyshev polynomial representation to construct a model of the restoring force:

$$f\left(x,\dot{x}\right) = \sum_{i=0}^{m}\sum_{j=0}^{n} C_{ij}T_i\left(x\right)T_j\left(\dot{x}\right) \tag{6.8}$$

with T_i being the Chebyshev polynomial term of order i. Chebyshev polynomials are orthogonal and their coefficients can be determined with an easier numerical integration.

An extension proposed in other papers [16,17] defines the XV (displacement-velocity) model as follows:

$$f\left(x,\dot{x}\right) \approx \hat{f}\left(x,\dot{x}\right) = \sum_{i=0}^{i_{\max}} B_i F_i\left(x,\dot{x}\right) \leftrightarrow \text{XV model} \tag{6.9}$$

Where B_i are unknown coefficients and F_i are a set of basis functions of the state variables. Several papers are devoted to problems that may arise in the application of these methods: from the potential lack of measured state variables, because usually only one state variable is directly measured, to the analysis of the type of excitation signal to be used to perform a better identification [16,18,19].

The RFS method is not directly applicable to certain types of nonlinear systems, and specifically to hysteretic systems, where the pattern of the hysteretic force is rate-independent. In this case, the restoring force derivative does not depend on the state

variables only, but also on the internal force itself. As already stated, the RFS of a hysteretic system is multi-valued if represented just by x and $\dot{x}$. Several authors proposed extensions of the RFS method in order to identify hysteretic systems. Among others, Benedettini *et al* [20] and Lo *et al* [21] proposed models of the following type:

$$\dot{f} = g\left(\dot{x}, f\right) \leftrightarrow \text{VF model} \tag{6.10}$$

where VF stands for Velocity-Force. Such models allow for a representation of the surface of the restoring force derivative in the plane $\left(\dot{x}, f\right)$. Also parametric approaches have been pursued [22]. Benedettini *et al* [20] and Masri *et al* [23] used an alternative approach by proposing a polynomial base approximation of the restoring force as a function of velocity, displacement and the excitation.

A further generalization of Equation (6.10), leads to the model used in this paper, consists of identifying a Duhem hysteretic model [24] as follows:

$$\dot{f} = g\left(x, \dot{x}, f\right) \leftrightarrow \text{XVF model} \tag{6.11}$$

where XVF stands for displacement, velocity, force. Once a mathematical model has been identified, it is possible to predict and simulate the behaviour of the system under different excitations. The identification of systems defined as Equation (6.10) and (6.11) can be viewed as extensions of the original RFS method (Equation (6.9)).
The method has been extended to MDoF systems by the same authors [25], by resorting to the representation of the dynamic equation of motion in modal coordinates. In fact, in the case of system described by the following equation:

$$\left[M\right]\cdot\left\{\ddot{x}\right\} + f\left(\left\{x\right\},\left\{\dot{x}\right\}\right) = \left\{u\right\} \tag{6.12}$$

where $\left[M\right]$ is the mass matrix, $f\left(\left\{x\right\},\left\{\dot{x}\right\}\right)$ contains the restoring actions for the different DoF, $\left\{x\right\}$ is the displacement vector and overdots represent time differentiation. One can rewrite equation (6.12) in terms of modal coordinates by pre-multiplying both sides of the equation by the matrix of the eigenvalues $\left\{\Psi\right\}$ of the underlying linear system:

$$\begin{aligned} &\left[m\right]\cdot\left\{\ddot{p}\right\} + h\left(\left\{p\right\},\left\{\dot{p}\right\}\right) = \left[\Psi\right]\cdot\left\{u\right\} \\ &h_i = u_{\text{mod},i} - m_i\ddot{p}_i = h_i\left(p_1,...,p_N,\dot{p}_1,...,\dot{p}_N\right) \end{aligned} \tag{6.13}$$

where $\left\{p\right\}$ is the vector of modal displacements, $\left[m\right]$ is the diagonal matrix of modal masses, h_i is the i$^{\text{th}}$ restoring force and $u_{\text{mod},i}$ is the exciting force acting on the i$^{\text{th}}$ mode. In such a case the components h_i are quantifiable in the same way as in the SDoF case. The modal matrix does not allow for the decoupling of the equation of motion but decoupling can be forced by using some corrective coefficients (see [25]).

6.2.3 NARMAX modelling

The NARMAX (Nonlinear AutoRegressive Moving Average with eXogenous inputs) method has been developed by Billings and others during a long time span [26,27,28]. It consists in the extension of autoregressive models with moving average model already applied in linear identification.

The method can be applied to a wide range of nonlinear systems as it is witnessed by the literature about the method [26,27,28].

A NARMAX model is a discrete approximation of the motion equation expressed in continuous form, and one can write the regressive model as:

$$x_i = F\left(x_{i-1}, x_{i-2}, ...x_{i-n_x}; u_{i-1}, u_{i-2}, ...u_{i-n_u}, \xi_{i-1}, \xi_{i-2}, ...\xi_{i-n_\xi}\right) + \xi \tag{6.14}$$

where F is a nonlinear function and x_i, u_i and ξ_i are the system response, the excitation and the noise at instant t_i, respectively. The subscripts n_x, n_u and n_ξ represents the maximum lags in the output, the input and the noise. In the case of a system polynomial by nature, equation (6.14) will approximate the model in a good fashion for all levels of excitation [26,27]. In the case of a not polynomial nonlinearity, the coefficients of (6.14) can approximate the system arbitrarily over a given range of their arguments but in such a case the model will be input sensitive due to the Weierstrass approximation theorem. In such a case, one can improve the fitting on the response of the system by adding non-polynomial terms to the regression [29].

Generally speaking the identification process can be performed by using a least square optimisation [28] or on the basis of the statistical characteristics of the model, in particular on the error reduction index [30]. Tao [31] proposed also an extension of the method in the case of "output-only" series.

The accuracy of the identified model is evaluated a posteriori, by checking if the model has prediction capabilities. Different validation tests have been proposed, but the most stringent is the correlation test. One can compute the cross-correlation function $\varphi(k)$ between the identified series and the predicted one. One has to check that the residual signal ξ is uncorrelated with the input sequence. If this condition is satisfied the NARMAX model is complete and can represent the behaviour of the system in an adequate fashion.

Billings *et al* [29] have shown that this condition is satisfied when the following relationships between auto- and cross-correlation function of the sequences $\{u_i\}$, $\{u_i^2\}$, $\{\xi_i\}$, $\{\xi_i^2\}$ hold:

$$\begin{cases} \varphi_{ee}(k) = \delta_{0k} \\ \varphi_{ue}(k) = 0, \ \forall k \\ \varphi_{e(eu)}(k) = 0, \ \forall k \geq 0 \\ \varphi_{u^2 e}(k) = 0, \ \forall k \\ \varphi_{u^2 e^2}(k) = 0, \ \forall k \end{cases} \tag{6.15}$$

6.2.4 Reverse Path method and Conditioned Reverse Path method

The time-domain is usually considered the standard domain in the field of nonlinear identification. Nonetheless, reverse path spectral methods were introduced in order to accommodate the presence of nonlinearities. In the nonlinear field the frequency response functions (FRFs) cannot lead to the identification of the modal parameters, because the FRFs in nonlinear field can change their parameters depending on the excitation level.

The Reverse Path method (RP) was firstly developed by Bendat *et al* [32] in order to identify nonlinear SDoF systems. Successively, Richards & Singh [33] introduced the Conditioned Reverse Path method (CRP) which allowed for a generalisation of the method for MDoF structures excited in a number of point less than the number of DoF.

The RP method requires to write the equation of motion as follows:

$$[M]\{\ddot{x}\} + [C]\{\dot{x}\} + [K]\{x\} + \sum_{j=1}^{n} [A]_j \{y\}_j = \{u\} \tag{6.16}$$

with $[M]$, $[C]$ and $[K]$ being respectively the mass, damping and stiffness matrixes, $\{x\}$ and $\{u\}$ the vector of displacement and of the excitation. The system may be characterised by different types of nonlinearities: they are considered by using n vectors $\{y\}_j$. The size of these vectors is $q_j \times 1$ and the terms describe the nonlinear relationship between the DoF and the internal restoring forces. For instance, in the case of polynomial nonlinearity one can write $\{y\}_j = \left\{\Delta x_k{}^{m_j}\right\}$ with Δx_k being the relative displacement between two DoF and m_j is the polynomial degree of the j^{th} vector. The matrixes $[A]_j$ identify the entity of the internal nonlinear forces and have size $N \times q_j$. By transforming both sides of equation (6.16) one can rewrite the equation of motion in the frequency domain:

$$\left[B_L(\omega)\right]\left\{X(\omega)\right\}+\sum_{j=1}^{n}\left[A\right]_j\left\{Y(\omega)\right\}_j=\left\{U(\omega)\right\} \tag{6.17}$$

where $\left[B_L(\omega)\right]=-\omega^2\left[M\right]+i\omega\left[C\right]+\left[K\right]$ is the dynamic stiffness matrix while $\left\{X(\omega)\right\}$, $\left\{U(\omega)\right\}$ and $\left\{Y(\omega)\right\}$ are the Fourier transforms of displacements, excitation and nonlinear terms $\left\{y(t)\right\}_j$, respectively.

The method takes its name after equation (6.17), where the excitation plays the "role" of output while the displacements act as input. By exploiting the difference in the representation of the input-output relationship and by using the matrix of FRFs, the RP method allows to distinguish between linear and nonlinear terms. Therefore, it is possible to determine auto- and cross-power spectral densities of displacements and excitations:

$$\begin{cases}\left[S_{XU}(\omega)\right]=\dfrac{2}{T}E\left[X(\omega)^*U(\omega)\right]=\left[S_{XX}(\omega)\right]\left[B_L\right]^T+\sum_{j=1}^{n}\left[S_{XY_j}(\omega)\right]\left[A\right]_j^T\\ \left[S_{Y_1U}(\omega)\right]=\dfrac{2}{T}E\left[Y_1(\omega)^*U(\omega)\right]=\left[S_{Y_1X}(\omega)\right]\left[B_L\right]^T+\sum_{j=1}^{n}\left[S_{Y_1Y_j}(\omega)\right]\left[A\right]_j^T\\ \ldots\\ \left[S_{Y_nU}(\omega)\right]=\dfrac{2}{T}E\left[Y_n(\omega)^*U(\omega)\right]=\left[S_{Y_nX}(\omega)\right]\left[B_L\right]^T+\sum_{j=1}^{n}\left[S_{Y_nY_j}(\omega)\right]\left[A\right]_j^T\end{cases} \tag{6.18}$$

Where $\left[S_{XU}(\omega)\right]$, $\left[S_{Y_1U}(\omega)\right]$, …, $\left[S_{Y_nU}(\omega)\right]$ are the power spectral density matrixes, E is the expected value operator, T is the length of the time window an * is the conjugation operator. Usually, equation (6.18) is employed in its matricial form:

$$\begin{cases} [\Gamma]=[\Xi]\cdot[\Psi]^T \\ [\Gamma]=\left[\left[S_{XU}(\omega)\right]^T \quad \left[S_{Y_1U}(\omega)\right]^T \quad \left[S_{Y_2U}(\omega)\right]^T \quad \dots \quad \left[S_{Y_nU}(\omega)\right]^T\right]^T \\ [\Xi]=\begin{bmatrix} \left[S_{XX}(\omega)\right] & \left[S_{UY_1}(\omega)\right] & \left[S_{UY_2}(\omega)\right] & \dots & \left[S_{UY_n}(\omega)\right] \\ \left[S_{Y_1X}(\omega)\right] & \left[S_{Y_1Y_1}(\omega)\right] & \left[S_{Y_1Y_2}(\omega)\right] & \dots & \left[S_{Y_1Y_n}(\omega)\right] \\ \left[S_{Y_2X}(\omega)\right] & \left[S_{Y_2Y_1}(\omega)\right] & \left[S_{Y_2Y_2}(\omega)\right] & \dots & \left[S_{Y_2Y_n}(\omega)\right] \\ \dots & \dots & \dots & \dots & \dots \\ \left[S_{Y_nX}(\omega)\right] & \left[S_{Y_nY_1}(\omega)\right] & \left[S_{Y_nY_2}(\omega)\right] & \dots & \left[S_{Y_nY_n}(\omega)\right] \end{bmatrix} \\ [\Psi]=\left[\left[B_L\right] \quad [A]_1 \quad [A]_2 \quad \dots \quad [A]_N\right] \end{cases} \tag{6.19}$$

Richard and Singh observed that the matrix $[\Xi]$ can be determined by inversion only in the cases with a number of excitations equal to the number of measured DoF of the system. In experimental cases, this condition is rarely satisfied, therefore equation allows only for determining the rows of $[\Xi]$ corresponding to the DoF where an excitation force acts. Moreover, the problem is characterised by numerical ill-conditioning because there is a strong correlation among the power spectral density of the nonlinear terms at the different frequencies.

The CRP method is based upon the determination of a certain number of uncorrelated input by using the conditioned power spectral densities. This approach overcomes the difficulties shown by RP method: the numerical problem in this case is well-conditioned and it can be applied also in the case in which the number of excited point is less than the number of measured DoF. On the other hand, the computation of conditioned power spectral densities is quite expensive. Numerical an experimental application were proposed by Bendat *et al* [34], Marchesiello *et al* [35], Garibaldi and Marchesiello [36], Kerschen and Golinval [37], Marchesiello [38].

6.2.5 Nonlinear identification through feedback and output (NIFO)

The NIFO technique has been proposed by Adams and Allemang [39,40,41] and it is based upon the concept of "feedback" of the output, namely the possibility to interpret the internal nonlinear restoring forces as a series of input acting on the corresponding linear system. These forces are functions of the system response and, if they are neglected,

introduce in the input/output relationship an effect which is similar to the one exercised by the noise in the structural response.

The formulation of the NIFO method is analogous to the one introduced for the Reverse Path method and it resorts as well to the dynamic stiffness to represent the dynamic equilibrium in the frequency domain. It is possible to distinguish among linear and nonlinear terms as follows:

$$\begin{aligned}\left[B_L(\omega)\right]\left\{X(\omega)\right\}+\sum_{j=1}^{n}\mu_j(\omega)\left\{B_{nj}\right\}X_{nj}(\omega)&=\left\{U(\omega)\right\}\\ \left[B_L(\omega)\right]\left\{X(\omega)\right\}&=\left\{U(\omega)\right\}-\sum_{j=1}^{n}\mu_j(\omega)\left\{B_{nj}\right\}X_{nj}(\omega)\end{aligned} \tag{6.20}$$

where $\left[B_L(\omega)\right]$ is the dynamic stiffness matrix and $\left\{X(\omega)\right\}$ and $\left\{U(\omega)\right\}$ are the Fourier transform of the system response and of the excitation force, respectively. The internal nonlinear restoring forces are expressed by the scalar functions $X_{nj}(\omega)$ while $\mu_j(\omega)$ represents the entity of these forces. $\left\{B_{nj}\right\}$ is a column vector (whose terms can assume the values +1, 0 or -1) which applies the respective j^{th} force $\mu_j(\omega)X_{nj}(\omega)$ to the corresponding DoF.

Unlike the RP method, which relies on a specific model for desribing the dynamic behaviour of the system, equation (6.20) does not require any assumption on the type of nonlinearity. The assumption is that any type of nonlinear internal actions can be expressed as a linear combination of the system response and the system excitation.

$$\begin{aligned}\left\{B_{nj}\right\}X_{nj}(\omega)&=\left[{}_xB_{nj}(\omega)\right]\left\{X(\omega)\right\}\\ \left\{B_{nj}\right\}X_{nj}(\omega)&=\left[{}_uB_{nj}(\omega)\right]\left\{U(\omega)\right\}\end{aligned} \tag{6.21}$$

$\left[{}_xB_{ni}(\omega)\right]$ and $\left[{}_uB_{ni}(\omega)\right]$ being the matrices which projects the j^{th} nonlinear vector in the output or input, respectively. This makes it possible to neglect the nonlinear feedback of the output, substituting it with quantities that are function of the measured data only.

By introducing equation (6.21) in (6.20) one has:

$$\begin{aligned}\left[B_L(\omega)\right]\left\{X(\omega)\right\}+\sum_{j=1}^{n}\mu_j(\omega)\left[{}_xB_{nj}(\omega)\right]\left\{X(\omega)\right\}&=\left\{U(\omega)\right\}\\ \left[B_L(\omega)\right]\left\{X(\omega)\right\}&=\left\{U(\omega)\right\}-\sum_{j=1}^{n}\mu_j(\omega)\left[{}_uB_{nj}(\omega)\right]\left\{U(\omega)\right\}\end{aligned} \tag{6.22}$$

Both members of equation (6.22) are multiplied by the matrix $\left[H_L(\omega)\right]=\left[B_L(\omega)\right]^{-1}$, which contains the FRF of the equivalent linear system. This leads to the formulation of the NIFO method:

$$\begin{aligned}\left\{X(\omega)\right\}&=\left[{}_xH_M(\omega)\right]\left[H_L(\omega)\right]\left\{U(\omega)\right\}\\ \left\{X(\omega)\right\}&=\left[H_L(\omega)\right]\left[{}_uH_M(\omega)\right]\left\{U(\omega)\right\}\end{aligned} \tag{6.23}$$

where:

$$\begin{cases}\left[{}_xH_M(\omega)\right]=\left(\left[I\right]+\left[H_L(\omega)\right]\sum_{j=1}^{n}\mu_j(\omega)\left[{}_xB_{nj}(\omega)\right]\right)^{-1}\\ \left[{}_uH_M(\omega)\right]=\left[H_L(\omega)\right]\left(\left[I\right]-\sum_{j=1}^{n}\mu_j(\omega)\left[{}_uB_{nj}(\omega)\right]\right)\end{cases} \tag{6.24}$$

$\left[{}_xH_M(\omega)\right]$ and $\left[{}_uH_M(\omega)\right]$ are called modulation matrices because they modulate the FRF of the equivalent linear system in order to adequately describe the input/output relation of the system. These matrices reflect the corresponding nonlinear systems: in detail, they are depending on the excitation level and are not symmetric. The NIFO method is not parametric; in fact it does not require any a priori assumption on the nature nor localisation of the nonlinearities. This information can be inferred from the modulation matrices. Experimental applications of this method are limited (see Kerschen and Golinval [37] or Garibaldi and Marchesiello [36]), therefore it is difficult to figure out direct applications of this method to full-scale structures.

6.2.6 Volterra series and higher order frequency response functions

The dynamic response $x(t)$ for a general SDoF time-invariant linear system to an external excitation $u(t)$ can be expressed by the Duhamel's integral or convolution integral:

$$x(t)=\int_{-\infty}^{+\infty}h(\tau)u(t-\tau)d\tau \tag{6.25}$$

where $h(t)$ is the impulse response function (IRF) or order 1 kernel. The IRF is zero for t<0 because in causal systems the response cannot depend on future values of the excitation force. Moreover, if $x(t)$ and $x(t-\tau)$ are the responses to the excitations $u(t)$ and $u(t-\tau)$ the system can be called time-invariant.

The extended form of (6.25) has been obtained by Volterra [42] and it is expressed by a series of functions. All the terms of the series are defined by generalising (6.25) with a convolution integral on a multidimensional domain:

$$\begin{aligned} x(t) &= x_1(t) + x_2(t) + ... + x_k(t) + ... \\ x_k(t) &= \int_{-\infty}^{+\infty} ... \int_{-\infty}^{+\infty} h_k(\tau_1, \tau_2, ..., \tau_k) u(t-\tau_1) ... u(t-\tau_k) d\tau_1 ... d\tau_k \end{aligned} \tag{6.26}$$

By $x_k(t)$ being the k^{th} term of the series, and where the function $h_k(t_1, t_2, ..., t_k)$ is called Volterra kernel or HIRF (Higher-order Impulse Response Function). Expression (6.25) simply represents the lowest-order truncation which is exact only for linear systems.

Schetzen [43] demonstrated that kernels can be considered symmetric without any loss of generality (i.e. $h_2(\tau_1, \tau_2) = h_2(\tau_2, \tau_1)$).

The expansion in Volterra series exists also in the frequency-domain. In such a case, one can define the HOFRF (Higher-Order Frequency Response Function) or Volterra kernel transforms as $H_k(\omega_1, ..., \omega_k)$:

$$H_k(\omega_1, ..., \omega_k) = \int_{-\infty}^{+\infty} ... \int_{-\infty}^{+\infty} h_k(\tau_1, ..., \tau_k) \cdot e^{-i(\omega_1\tau_1 + ... + \omega_k\tau_k)} d\tau_1 ... d\tau_k \tag{6.27}$$

In the frequency domain, the system response will be given by the following set of equations:

$$\begin{aligned} Y(\omega) &= Y_1(t) + Y_2(t) + Y_3(t) ... \\ Y_1(\omega) &= H_1(\omega) X(\omega) \\ Y_2(\omega) &= \frac{1}{2\pi} \int_{-\infty}^{+\infty} H_2(\omega_1, \omega - \omega_1) X(\omega_1) X(\omega - \omega_1) d\omega_1 \\ &... \end{aligned} \tag{6.28}$$

One of the main uses of Volterra series is the construction of analytic approximation to various quantities of interest in structural analysis. The approximation of the FRFs for SDoF and MDoF systems with cubic nonlinearities and excited by Gaussian noise can be found in [44,45]. The approximations derived are of interest because the FRFs constructed have all their poles in the upper-half of the complex frequency plane. This explains why the FRFs of randomly excited nonlinear systems appear to be invariant under the Hilber transform. The HOFRFs can be expressed analytically with the method of the harmonic probing (see [3]).

It is worth mentioning also the approximated solution method proposed by Vasquez *et al* in [46,47] and recently extended to MDoF systems [48]. They proposed to

model the behavior of the Volterra operators by linear equations that map the kth-order operator from an excitation of the same order produced by a combination of lower-order operators. This group of equations is called Associated Linear Equations (ALEs). The main advantage of this approach is that the nonlinear system is represented as a series of linear system and the theory developed for linear systems may be used. This approach has been applied also in the identification of hysteretic systems using polynomial forms, see for instance the works by Demarie *et al* [49] or [50].

Volterra [42] series is an interesting means of establishing a non-parametric model of a nonlinear input-output process. Moreover, the kernel transforms allows identifying and interpreting interactions between input frequencies and give a visualization equivalent to the Bode plot for linear systems. The main limitation of this approach is the existence and convergence of the series. Many nonlinearities of practical interest have discontinuous or non-smooth nonlinearities and the corresponding systems do not strictly have a Volterra representation. A related problem is that the radius of the convergence of the series may be restricted or that low-order truncations may not be accurate.

6.2.7 Neural Networks

Another possible approach to nonlinear identification, completely alternative to the methods aforementioned, is the "black-box" approach. In such approach, one can completely avoid the physical modelling but the only aim of the method is to describe the functional link between input and output of the system. In this framework, in the last decades more importance has been given to neural networks, because they can approximate continuous functions with different levels of accuracy. The exposition of the theory of neural networks does not fit with the purpose of this thesis, and for brevity's sake, only a review of the principal application of neural networks in nonlinear identification will be made. For an extensive dissertation on neural networks, one can see [51].

A neural network is a mathematical object which can reproduce the input-output relationship of a system. The network is composed generally of different elementary object, called neurons, disposed on different layers, and connected among them in order to reproduce a simplified neurobiological network (see figure 6.2).

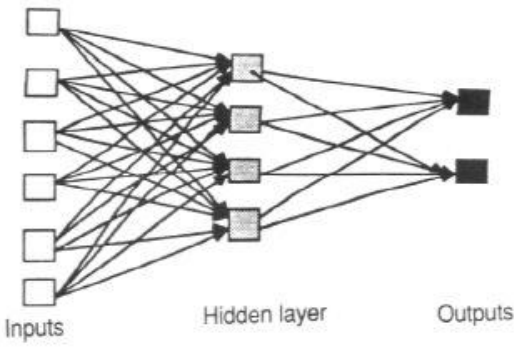

Figure 6.2 - Simplified scheme of feed-forward Neural Network

The single neurons can process only one data at a time, and can make operations of weighting and threshold on the data. The connections between neurons can be linked to some weights, which are determined during the "training" phase of the network. In fact, neural networks are adaptive systems which can learn and improve their accuracy.

Once the structure of the network is defined (type, number of neurons and number of connections) and it is trained (value of the weighting coefficients) one can use the network to predict the response of the system. Since the 80s a lot of efforts have been made in order to use these tools in the field of identification, control and diagnosis of structures. The most relevant works are those of Chen [52] and Masri [53]. The most common used neural networks are of the type "Multi-Layer Perecptron" (MLP) and "Radial Basis Function" (RBF). The first type has been used together with NARMAX modelling by Billings *et al* [54,55] and in order to identify the internal restoring forces (see Masri [53]), while the latter have been used in the experience of Chen [52]. Furthermore, Wray & Green in [56] demonstrated that exist a correlation between the weighting coefficients of neural networks and higher FRF of the modelled system.

It is worth mentioning the importance of neural networks in the framework of structural diagnostic, which is usually the successive phase with respect to identification. Anyway, in diagnostic empirical approaches are usually preferred in comparison to symptomatic approaches (see [57]), and they exploit the discerning capability of neural networks more than their capability to identify the systems.

On the other hand, the symptomatic approach can be used in order to detect the type of nonlinearity and to choose the better suited identification method.

6.3 Instantaneous and on-line methods for nonlinear identification

In this section a review of instantaneous nonlinear identification methods will be made. Some of the principal methods will be successively analysed and explained also by using numerical examples.

In structural dynamics it is often useful to detect changes in the modal (or model) parameters. Moreover, a simple way to check the consistency of a given model consists of

extracting instantaneous estimates of the model parameters. This may be obtained via standard identification methods applied sequentially on blocks or subsets of the full data so one can detect whether the parameters change slowly with time, or better by applying instantaneous approaches, which provide estimates of quantities that are inherently time-varying (e.g. an instantaneous frequency, degradation in stiffness or strength etc.). Approaches based on instantaneous estimation had been already considered in the 1960s for problems in acoustics and vibrations [58], but it is only from the 1990s that they gained widespread popularity within the structural dynamics community. A survey of the analysis of non-stationary signals using time-frequency methods is available in Hammond and White [59], Hammond and Waters [60], Ceravolo [61].

Feldman showed how to use the traditional definition of the analytic signal and the time-domain Hilbert transform in order to identify nonlinear models of SDOF systems. The FREEVIB and FORCEVIB (see 6.3.1 for further details) approaches can be used to construct the instantaneous damping and stiffness curves for a large class of nonlinear systems, but are only suitable for single component signals [62]. A method for the decomposition of signals with multiple components into a collection of single component signals, termed intrinsic mode functions (IMFs), was proposed in Huang *et al* [63] and is now referred to as the Hilbert-Huang transform in the time-frequency literature. The IMFs are constructed such that they have the same number of extrema and zero-crossings, and only one extremum between successive zero-crossings. As a result, they admit a well-behaved Hilbert transform. The method now has several applications in structural dynamics including linear system identification [64,65] and damage detection [66].

Other time-frequency representations are also suitable for the analysis of nonlinear oscillations. Linear representations have been used, for instance, by Spina *et al* [67] and Demarie *et al* [49]. An overview of the use of the wavelet transform in nonlinear dynamics can be found in Staszewski [68], while interesting applications are reported by Newland [69] and Erlicher and Argoul [70] among others. Quadratic representations which include the Wigner-Ville distribution and the Cohen-class of distributions have also received some attention [71,72,73].

Today, the instantaneous identification of the parameters of a system is a suitable way to detect and quantify a degradation or damage. Unfortunately, not all instantaneous approaches admit an on-line or real-time implementation which, for instance, is necessary in structural control. In other words, on-line methods do not require the acquisition process to be completed to perform the identification, while off-line methods retain this limitation. Despite leading to instantaneous or time-varying parameters, a time-frequency method cannot be strictly termed a real-time approach (see for instance [74]). In fact, at least in theory, the time-frequency uncertainty principle does not allow for an on-line implementation [61,75]. This said, in actual practice the choice of using on-line or off-line predictions depends on the type of transform: an analysis based on running windows (as in the case of the spectrogram) can loosely support an on-line implementation, unlike a correlative transform structure (e.g. Wigner-Ville transform).

In the time domain, the least squares approach is not always practical for on-line identification of the parameters of a nonlinear system, even if it is possible to find some important examples in literature [76]. Many other identification methods have been investigated: the Extended Kalman Filter (EKF) [77,78,79,80,81,82], the H_∞ filter [83], or Sequential Monte Carlo (SMC) methods [84,85,86]. Andrieu *et al* [87] states that the

advent of SMC, due to good approximation of the optimal filter under weak assumptions, does not mean that SMC is the best candidate for on-line implementations. In fact SMC methods (also referred as particle filters) suffer from the so-called "degeneracy problem" and are also computationally expensive. Instead, the EKF procedure, which is currently the most exploited, derives from the state-space formulation of the differential equation of motion. The main advantage is that the EKF technique has seen several applications. In this procedure, the estimation problem is linearized using an extended state space representation of the system. The initial guess is then updated recursively when new observations are available. A family of auto-regressive moving average (ARMA) model have been investigated by Fassois *et al* [88,89], applied to the identification of time-varying systems. In the same connection, Xiuli and Wang [90] proposed a Gaussian multivariate variation of ARMA model.

We should also mention the recent work of Wu and Smyth [74], who have successfully applied the Unscented Kalman Filter (UKF) for on-line identification of parameters of hysteretic SDoF systems with both degrade in term of stiffness and strength and pinching. The Unscented Kalman Filter is a technique which allows dealing with nonlinear systems and it is able to deal with any type of nonlinearity with respect to the EKF. In detail, UKF does not require the computation of the Jacobian of the nonlinear function; in fact it does not approximate the measurement equation of the system but it approximates the posterior probability density by a Gaussian density, by using a set of deterministic points (the so-called Sigma points). When the Sigma points are propagated through the nonlinear transform, they capture the mean and the covariance of the system. Xie and Feng [91] proposed to use a further development of the UKF, the Iterated Unscented Kalman Filter (IUKF) to nonlinear and hysteretic springs. In this last case, also 2DoF systems with polynomial nonlinearities were investigated. The main advantage of these techniques when applied to hysteretic systems is their capability to deal with any type of functional nonlinearity.

6.3.1 Hilbert transform

The frequency-domain Hilbert transform has been used for nonlinearity detection, but a time-domain implementation of the method have been introduced in the field of nonlinear identification with two different approaches which were proposed by Feldman in [92] and in [93]: one is based on systems subject to free oscillations (FREEVIB) and one on systems subject to forced vibration (FORCEVIB).

The analytic signal can be computed for a large number of processes and it is defined by calculating the Hilbert transform of a signal. Accordingly, the signal can be represented as a combination of two slow varying functions called envelope and instantaneous phase [58,94]:

$$X(t) = x(t) - \mathcal{H}\{x(t)\} = x(t) - \tilde{x}(t) = A(t)e^{i\Psi(t)}$$

$$\begin{cases} A(t) = \sqrt{x(t)^2 - \tilde{x}^2(t)} \\ \Psi(t) = \arctan\left(\dfrac{\tilde{x}(t)}{x(t)}\right) \end{cases} \tag{6.29}$$

where $x(t)$ is the vibration of a generic system, $\mathcal{H}$ and $\tilde{x}(t)$ represent its Hilbert transform, $X(t)$ denotes the analytic signal and $A(t)$ and $\psi(t)$ are the envelope and the instantaneous phase, respectively.

The Hilbert transform, differently from the Fourier transform, transform a process remaining in the same domain and can be generally defined by the following:

$$\mathcal{H}\{x(t)\} = \tilde{x}(t) = -\frac{1}{i\pi} PV \int_{-\infty}^{+\infty} \frac{x(\tau)}{\tau - t} d\tau \tag{6.30}$$

The nonlinear behaviour of processes can be noticed by the link between frequency and damping to the amplitude of the excitation. This has lead Feldman to the use of the previously defined analytic signal and the concepts of instantaneous frequency and damping. In fact, by resorting to the concept of instantaneous phase, one can define the instantaneous frequency [95]:

$$\omega(t) = \dot{\psi}(t) = \frac{x(t)\dot{\tilde{x}}(t) - \dot{x}(t)\tilde{x}(t)}{x(t)^2 - \tilde{x}(t)^2} = \mathrm{Im}\left[\frac{\dot{X}(t)}{X(t)}\right] \tag{6.31}$$

The FREEVIB [92] method has been formulated in the case of SDoF system with free oscillations:

$$\ddot{x} + h(A)\dot{x} + \omega_0^2(A)x = 0 \tag{6.32}$$

where $x(t)$ is the system solution, overdots represent time derivatives, $h(A)$ represents the nonlinear damping function and $\omega_0^2(x)$ represents the nonlinear stiffness function. Feldman assumes that the functions $h(A)$, $\omega_0^2(A)$ and the structural response $x(t)$ have non-overlapping Fourier spectra: this is usually verified because whilst the first two are lowpass the latter is generally highpass. The main consequence of these assumptions is the invariance of $h(A)$ and $\omega_0^2(A)$ with respect to the Hilbert operator which leads to the following differential relationship:

$$\ddot{\tilde{x}} + h(A)\dot{\tilde{x}} + \omega_0^2(A)\tilde{x} = 0 \tag{6.33}$$

One can substitute equation (6.29) in (6.33) and it is possible to obtain the dynamic equilibrium in terms of the analytic signal:

$$\ddot{X} + h(A)\dot{X} + \omega_0^2(A)X = 0 \tag{6.34}$$

The derivatives of the analytic signal can be defined by resorting to equation (6.29):

$$\begin{cases} \dot{X}(t) = X(t)\left[\dfrac{\dot{A}(t)}{A(t)} + i\omega(t)\right] \\ \ddot{X}(t) = X(t)\left[\dfrac{\ddot{A}(t)}{A(t)} + \omega(t)^2 + 2i\dfrac{\dot{A}(t)\omega(t)}{A(t)} + i\dot{\omega}(t)\right] \end{cases} \tag{6.35}$$

Consequently, one can obtain the analytic expressions of the nonlinear stiffness and damping, which are the basis of the FREEVIB method:

$$\begin{cases} h(t) = -2\dfrac{\dot{A}(t)}{A(t)} - \dfrac{\dot{\omega}(t)}{\omega(t)} \\ \omega_0^2(t) = \omega^2(t) - \dfrac{\ddot{A}(t)}{A(t)} + 2\left(\dfrac{\dot{A}(t)}{A(t)}\right)^2 + \dfrac{\dot{A}(t)\dot{\omega}(t)}{A(t)\omega(t)} \end{cases} \tag{6.36}$$

In the case of free damped vibrations the amplitude $A(t)$ is a decreasing monotonic function therefore the inverse function $t(A)$ can be defined. One can therefore determine the instantaneous damping and instantaneous frequency in function of the amplitude: $h(A) = h(t(A))$ and $\omega_0^2(A) = \omega_0^2(t(A))$. The plot of amplitude versus instantaneous frequency is usually indicated as "backbone diagram".

The FORCEVIB [93] method was proposed as an extension of the previous method in the case of forced vibration. In this case, the dynamic equation of motion for an analytic signal is the following:

$$\ddot{X} + h(A)\dot{X} + \omega_0^2(A)X = \frac{U(t)}{m} \tag{6.37}$$

with m being the mass of the system (assumed to be known) and $U(t)$ is the analytic signal corresponding to the excitation force $u(t)$.

With the same assumptions made for the FREEVIB method, one obtains:

$$\begin{cases} h(t) = \dfrac{\beta(t)}{m\omega(t)} - 2\dfrac{\dot{A}(t)}{A(t)} - \dfrac{\dot{\omega}(t)}{\omega(t)} \\ \omega_0^2(t) = \omega^2(t) + \dfrac{\alpha(t)}{m} - \dfrac{\beta(t)\dot{A}(t)}{mA(t)\omega(t)} - \dfrac{\ddot{A}(t)}{A(t)} + 2\left(\dfrac{\dot{A}(t)}{A(t)}\right)^2 + \dfrac{\dot{A}(t)\dot{\omega}(t)}{A(t)\omega(t)} \\ \dfrac{U(t)}{X(t)} = \alpha(t) + i\beta(t) = \dfrac{u(t)x(t) + \tilde{u}(t)\tilde{x}(t)}{x^2(t) + \tilde{x}^2(t)} + i\dfrac{\tilde{u}(t)x(t) - u(t)\tilde{x}(t)}{x^2(t) + \tilde{x}^2(t)} \end{cases} \tag{6.38}$$

where $\alpha(t) = \mathrm{Re}\left[U(t)/X(t)\right]$ and $\beta(t) = \mathrm{Im}\left[U(t)/X(t)\right]$. The case $\left(\alpha(t) = \beta(t) = 0\right)$ is a particular case of (6.38) when it becomes equal to equation (6.36), therefore it renders the FREEVIB method as a particular case of the FORCEVIB method.

This method has been applied, due to its simplicity, with some success to experimental data particularly in the mechanical field [96]. In within the Civil Engineering framework, it is worth mentioning the works of Petrangeli [97] and De Stefano [98].

6.3.2 Instantaneous identification with time-frequency estimators

The concept of instantaneous identification with time-frequency representations has already been proposed in [61] and already applied to nonlinear oscillators in [99] or to experimental structures in [100,101].

To start with, in the time domain the identification of a parameters vector $\{p\}$ might be performed in the time domain [22] by minimising an error function ε(p),

$$\varepsilon(\{p\}) = \int_{-\infty}^{+\infty}\left[\left|v(t,\{p\})\right| - \left|v_m(t)\right|\right]^2 dt \longrightarrow \{p\}_{id} = \arg\left[\min_{\forall\{p\}} \varepsilon(\{p\})\right], \tag{6.39}$$

where v is a general state variable (displacement, acceleration, etc…), namely a nonlinear function of $\{p\}$, whilst v_m is the corresponding measured response, both functions of t.

However, the optimisation process defined via (6.39) lacks frequency localisation, i.e. it cannot use direct information about the localisation in time of harmonic components. As a result, to localise the nonlinear evolution of system parameters both in frequency and time [61], we define the error function as follows,

$$\varepsilon(t,\{p\}) = \left|\int_{-\infty}^{+\infty}\left[\tilde{T}_{\ddot{x}}(t,f;\{p\}) - T_{\ddot{x}_m}(t,f)\right]df\right| \longrightarrow \{p\}_{id}(\bar{t}) = \arg\left[\min_{\forall\{p\},t=\bar{t}} \varepsilon(t,\{p\})\right] \tag{6.40}$$

where $T_{\ddot{x}}(\ )$ denotes the time-frequency transform operator applied to the acceleration variable $\ddot{x}$. At any instant $\bar{t}$, the minimisation process leads to an associated optimal vector $\{p\}_{id}(\bar{t})$, which supplies instantaneous estimates of the model parameters. Notice

that the time-frequency transform could also be applied to the displacement x or any other state variable.

In this case the time-frequency representation was given a spectrogram form [75]. The instantaneous identification is based on the following minimisation at the discrete time [99,61]:

$$\varepsilon\left(j,\{p\}\right)=\left|\sum_{k=0}^{N-1}\left[SPEC_{x}^{(\gamma)}\left[j,k;\{p\}\right]-SPEC_{x_m}^{(\gamma)}\left[j,k\right]\right]\right| \longrightarrow \{p\}_{id}\left(\bar{t}=\bar{j}\Delta t\right)=\arg\left[\min_{\forall\{p\},j=\bar{j}}\varepsilon\left(j,\{p\}\right)\right] \tag{6.41}$$

where $\{p\}=\{m\ \alpha_1\ \alpha_2\ \alpha_3\ \cdots\ \alpha_n\}$ is the vector of parameters, referred to a general model capable to describe the dynamics of the identified system. $\mathrm{SPEC}_{x_m}^{(\gamma)}\left[j,k\right]$ and $\mathrm{SPEC}_{x}^{(\gamma)}\left[j,k;\{p\}\right]$ are the values of the spectrogram of the displacement x (or acceleration, etc…) at a discrete time instant $j\cdot\Delta t$ and frequency $k\cdot\Delta f$, respectively measured and calculated, while γ is a short time analysis window and N is the number of frequency samples. In recent published articles the authors have investigated the problems related to the choice of the optimal window analysis [61,102,75].

The "error function" ε provides the modulus of the difference between the instantaneous energy of the measured response x_m and that of the system output x corresponding to a given configuration of the unknown parameter vector p. By resorting to optimisation procedures, one can determine the minimum value of $\varepsilon\left(j=\bar{j},\{p\}\right)$ at every instant.

In some circumstances the system's response x may be calculated using Volterra series representations, this being convenient from the computational point of view [99]. Anyway, in the following examples the numerical response is calculated by solving the dynamic equation via a Runge-Kutta algorithm, in order to avoid limitations imposed by the type of nonlinearity.

6.3.2.1 Polynomial identification in the time-frequency domain

The first numerical investigations discussed here concern the identification strategy proposed by Masri *et al* [23,11]. Masri *et al* [23] state that the nonlinear or possibly hysteretic restoring force can be approximated by a polynomial function of the state variables of the system (XV type restoring force), with constant coefficients.

The form used for the simulations retains polynomial terms up to the 3rd order:

$$\begin{cases} m\ddot{x}+f=u(t) \\ f=\alpha_1\cdot x+\alpha_2\cdot\dot{x}+\alpha_3\cdot x^2+\alpha_4\cdot\dot{x}^2+\alpha_5\cdot x\dot{x}+\alpha_6\cdot x^2\dot{x}+\alpha_7\cdot x\dot{x}^2+\alpha_8\cdot x^3+\alpha_9\cdot\dot{x}^3 \end{cases} \tag{6.42}$$

The identification problem reduces to the estimation of the time-variant coefficients α in Equation (6.42). In this case the vector {p} reads: $\{p\}=\{\alpha_1,...,\alpha_9\}$. The instantaneous identification is based on the minimisation of the error function defined by

Equation (6.41) (the restoring force *f* has been chosen among the state variables to define the penalty function). The minimisation has been performed by using a Pattern Search algorithm [103]. Pattern Search algorithms allow generally for a fast convergence of the solution, and they are a good choice in problems where is required to locate the global maximum of the solution. Generally, for each minimisation, a maximum of 1000 evaluations of the cost function has been set in the following simulations.

In the simulations proposed afterwards it is generally assumed that the external excitation as well as the mass *m* are known. Although polynomials are often associated to non-parametric identification, some terms of the polynomial may retain a physical meaning, e.g. coefficients α_1 and α_2 of Equation (6.42) clearly represent a linearized stiffness and a viscous damping, respectively.

6.3.2.1.1 Example 1: Instantaneous identification of a SDoF system with Duffing nonlinearity under random excitation

In the first numerical example, a single degree of freedom (SDOF) system with Duffing nonlinearity is identified on an instantaneous base.

The system is excited by a stationary random process $n(\mu,\sigma)$, characterised by zero mean and a standard deviation σ=1.0. The sampling frequency of the random process is 100 Hz, and the length of the process is of 40 s. The parameters of the system characterise an underlying linear system with a frequency of 1 Hz. The system is defined by the following differential equation:

$$m\ddot{x} + c\dot{x} + kx + k_{nl}x^3 = u(t) \tag{6.43}$$

The system's real parameters are reported in table 6.2 together with the initial guesses for each parameter, while time histories are plotted in figure 6.3. As previously stated, the minimisation procedure is performed via a Pattern Search algorithm and parameters are bounded in a reasonable interval defined in table 6.2 as well.

Parameter	**m [kg]**	**c**	**k [N/m]**	**k_{nl} [N/m^3]**
Value	0.0253	0.0159	1.0	0.1
Initial guess	fixed	0.01	0.8	0
Lower bound	fixed	0	0.5	0
Upper bound	fixed	0.05	1.5	1

Table 6.2 - Duffing system parameters

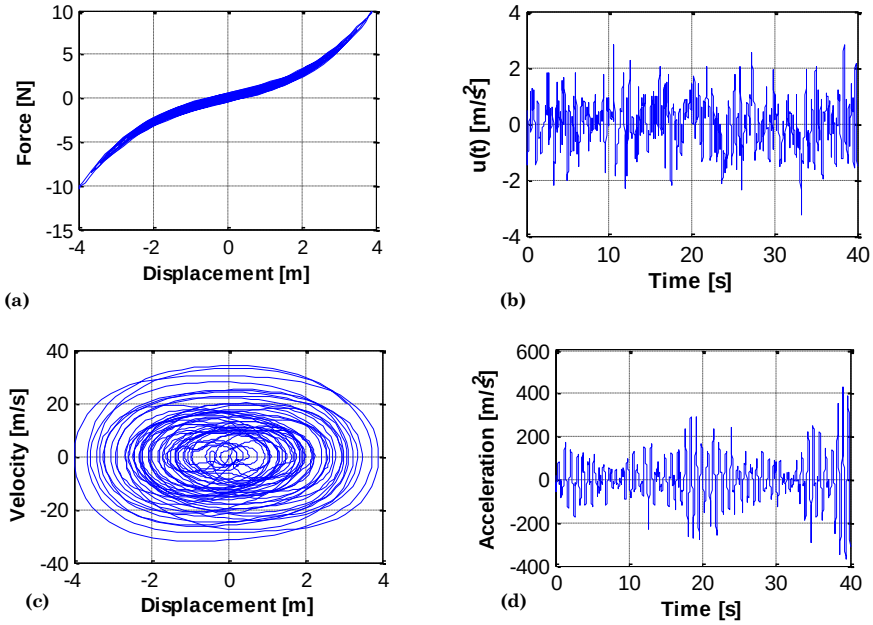

Figure 6.3 - Duffing oscillator: (a) phase plot of restoring force versus displacements; (b) input time history; (c) phase space; (d) acceleration time history

Through the identification process described by Equation (6.41), the polynomial coefficients have been identified instant by instant (analysis window used for the spectrogram: 400 samples, equivalent to 4 complete cycles of the response of the system, in order to minimise noise). In order to calculate the response of the identified system, estimates supplied at each time instant j by Equation (6.41) were averaged over smaller time intervals (1 s long).

The two time-history signals, measured and identified, show a good agreement. In order to give an index of the quality of the results, the Normalized Root Mean Squared (NRMS) error is introduced:

$$\mathrm{NRMS} = \frac{\sqrt{\dfrac{\sum_i \left(\hat{x}_i - x_i\right)^2}{n}}}{x_{\max}} \tag{6.44}$$

The NRMS errors for each one of the state variable are listed in table 6.3. It is possible to notice that the quality of fitting is good; in fact none of the errors is above the 1%.

NRMS	x	$\dot{x}$	$\ddot{x}$	f
Value	0.62%	0.35%	0.73%	0.77%

Table 6.3 - NRMS error of the different state variables for the Duffing system.

The instantaneous coefficients evaluated through this model, defined in Equation(6.42), in the case of a Duffing oscillator have a physical meaning. In fact the coefficient a_8 is the nonlinear stiffness, whilst a_1 and a_2 define the linear stiffness and the viscous damping.

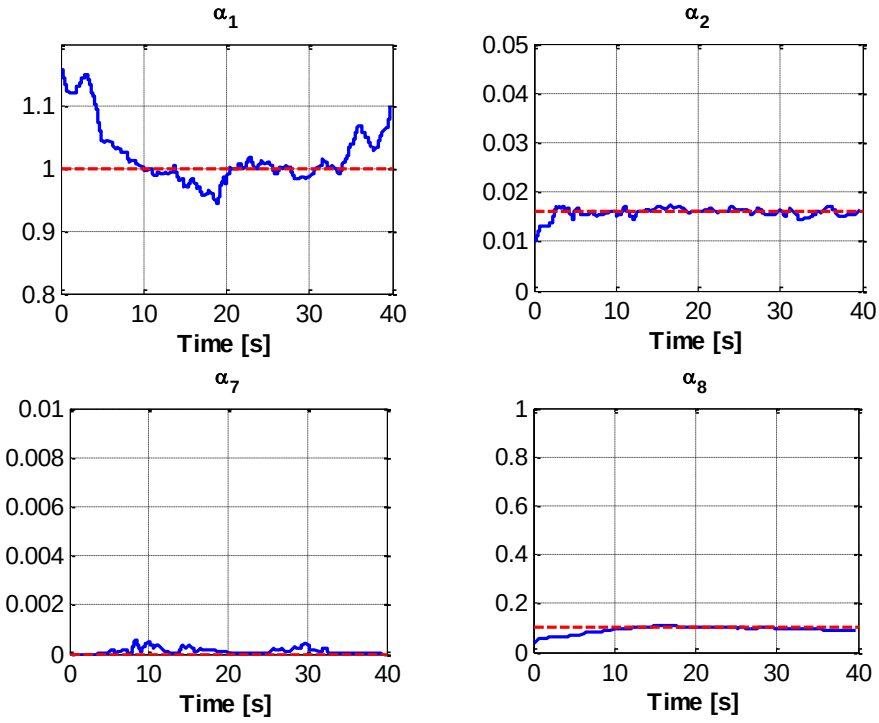

Figure 6.4 - Instantaneous coefficients identified (the straight dashed line represents the real value of the parameter): linear stiffness α1, viscous damping α2, Van der Pol term α7 (which should be 0), nonlinear stiffness cubic term α8.

Results in figure 6.4 show the instantaneous values of the estimated parameters in the exposed case of a Duffing oscillator. It is interesting to point out that only the parameter that are expected to have a value are activated by the optimisation process, while, for instance, the Van der Pol term α_7 is not activated significantly. Furthermore, the identification process reaches the exact value of the parameters after a few seconds and then stabilises. This may be not obvious because Equation (6.41) does not directly allow for correlation between the parameters estimated at each analysis window; anyway, the values of the parameters identified at the previous time block are used as initial guess

for the following step. This allows for a stabilisation of the results in the case of constant values of the real parameters.

6.3.2.1.2 Example 2: Instantaneous identification of a Duffing-Van der Pol oscillator with time-varying nonlinearity under random excitation

In this second example, a Duffing-Van der Pol oscillator will be identified. The system is defined by the following differential equation:

$$m\ddot{x} + c\dot{x} + kx + k_{nl,1}(t)x^3 + k_{nl,2}x^2\dot{x} = u(t) \tag{6.45}$$

The nonlinear coefficient $k_{nl,1}$ is assumed to vary linearly in time from a value $k_{nl\_init,1}$ to $k_{nl\_fin,1}$. The values assumed by the parameters of the system are listed in table 6.4 together with their initial guesses for the identification process.

Parameter	**m [kg]**	**c**	**k [N/m]**	**$k_{nl\_init,1}$ [N/m³]**	**$k_{nl\_fin,1}$ [N/m³]**	**$k_{nl,2}$ [N/m³/s]**
Value	0.0253	-0.0253	1.0	0.005	-0.005	0.00796
Initial guess	fixed	0	0.8	0	//	0
Lower bound	fixed		0.5		//	0
Upper bound	fixed		1.5		//	1

Table 6.4 - Duffing-Van der Pol system parameters

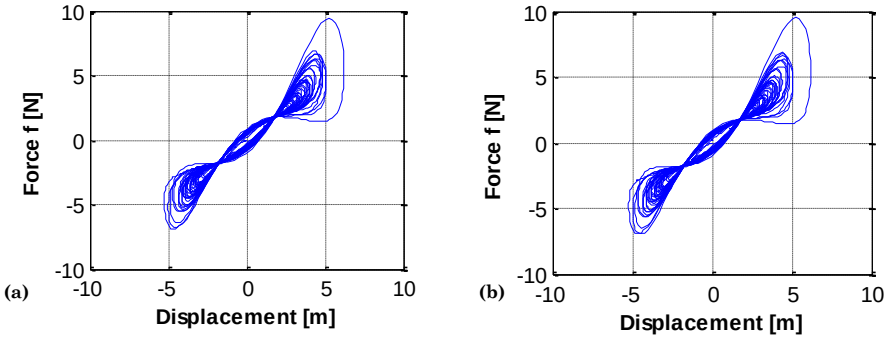

Figure 6.5 - Exact and estimated response for a system characterised by Duffing Van der Pol nonlinearity: (a) Exact force-displacement loop, (b) Identified force-displacement loop

Also in this case, the system is excited by the white Gaussian used for the previous example, noise characterised by μ=0.0 and σ=1.0 and the polynomial coefficients introduced by (6.42) have been identified minimising Equation (6.41).

Figure 6.5 shows the outcomes of the identification process. Apparently the model performs well in terms of fitting both the nonlinear restoring force and the phase plot of displacement and force.

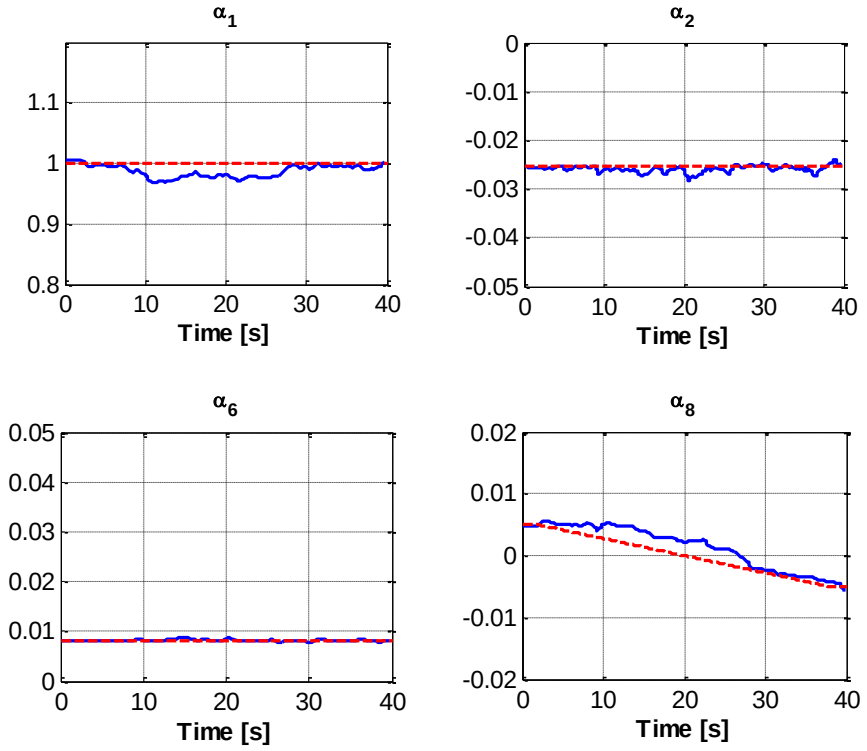

Figure 6.6 - Instantaneous coefficients identified (the straight dashed line represents the real value of the parameter): linear stiffness α1, viscous damping α_2, nonlinear Van der Pol term α_6, nonlinear stiffness cubic term α_8

In the case of the Duffing-Van der Pol oscillator the coefficients α_6 and α_8 assume the values of the nonlinear terms, while the coefficients α_1 and α_2 define respectively the linear stiffness and the viscous damping of the system. In fact, figure 6.6 highlights that the linear trend of the coefficient α_8 is captured by the algorithm. The NRMS error in terms of displacement and force is 0.50% and 0.31%, respectively.

6.3.2.2 Instantaneous identification of a $\dot{f}=g(x,\dot{x},f)$ polynomial form

Benedettini *et al* [20] observed that a $f = g(x,\dot{x})$ form for the restoring force is not suitable in the presence of hysteresis, which is typical of engineering structures. This is made evident when considering a hysteretic formulation such as the Bouc-Wen model [104,105,106]:

$$\begin{cases} m\ddot{x} + f = u(t) \\ \dot{f} = \left[A - |f|^n \left(\beta \cdot \mathrm{sgn}(f \cdot \dot{x}) + \gamma \right) \right] \dot{x} \end{cases} \tag{6.46}$$

In Equation (6.46) the parameter A is the linear stiffness of the oscillator, β>0, $\gamma \in [-\beta, \beta]$ and n>0 are constants affecting the form of the hysteresis loops. When n is large enough, force-displacement loops are similar to those of an elastic-perfectly-plastic model. Despite its simplicity and the fact that it fulfils the 2nd principle of thermodynamics, the Bouc-Wen model is affected by the so-called "violation of the Drucker-Prager postulate". A comprehensive discussion of these topics is presented in [107,108] and [109].

In the case of Equation (6.46) a XVF model can be used for the identification process. For identification purposes, Equation (6.42) is rewritten with the polynomial terms up to the 3rd order as follows:

$$\begin{cases} m\ddot{x} + c\dot{x} + f = u(t) \\ \dot{f} = \alpha_1 x + \alpha_2 \dot{x} + \alpha_3 f + \alpha_4 x^2 + \alpha_5 \dot{x}^2 + \alpha_6 f^2 + \alpha_7 x\dot{x} + \alpha_8 xf + \cdots \\ \qquad \cdots + \alpha_9 \dot{x} f + \alpha_{10} x\dot{x} f + \alpha_{11} x^2 \dot{x} + \alpha_{12} x\dot{x}^2 + \alpha_{13} x^2 f + \cdots \\ \qquad \cdots + \alpha_{14} x f^2 + \alpha_{15} \dot{x}^2 f + \alpha_{16} \dot{x} f^2 + \alpha_{17} x^3 + \alpha_{18} \dot{x}^3 + \alpha_{19} f^3 \end{cases} \tag{6.47}$$

What is crucial for the identification process is selecting the dominant polynomial terms. Actually, in most cases a polynomial form with a limited number of dominant terms ensures a good fitting, while the other terms can be set equal to zero.

6.3.2.2.1 Example 3: Instantaneous identification of a SDoF system with Duffing nonlinearity under random excitation

In Example 1 (6.3.2.1.1), a XV polynomial approximation has been used to identify a system characterised by a Duffing nonlinearity. The same system will be hereinafter identified through the more general XVF polynomial. So, in this case, the identification process consists of extracting punctual estimates for the polynomial coefficients in Equation (6.47). It is worth remarking that in most engineering applications only odd polynomial terms are considered, hence a simpler XVF polynomial approximation has been used in the following:

$$\begin{cases} m\ddot{x} + c\dot{x} + f = u(t) \\ \dot{f} = \alpha_1 x + \alpha_2 \dot{x} + \alpha_3 f + \alpha_4 x\dot{x} f + \alpha_5 x^2 \dot{x} + \alpha_6 x\dot{x}^2 + \alpha_7 x^2 f + \cdots \\ \qquad \cdots + \alpha_8 x f^2 + \alpha_9 \dot{x}^2 f + \alpha_{10} \dot{x} f^2 + \alpha_{11} x^3 + \alpha_{12} \dot{x}^3 + \alpha_{13} f^3 \end{cases} \tag{6.48}$$

While in the previous example the viscous damping was estimated directly as a part of the polynomial form, the new formulation in terms of restoring force derivative does not allow a direct estimation (there are no polynomial terms depending on acceleration). In this case, viscous damping must be evaluated separately from the polynomial coefficients that approximate the restoring force derivative.

Figure 6.7 shows the estimated instantaneous values of the coefficients and highlights that estimates of polynomial terms that are not included in the Duffing model are stable around zero (only a_4 term is reported for brevity's sake). Consider that, when working in terms of $\dot{f}$, the exact value for a_5 is three times the cubic nonlinear stiffness reported in table 6.2. In this case the NRMS error is of 0.89% for displacement and 0.48% for the force which is comparable to the error given by the XV model (Table 6.3).

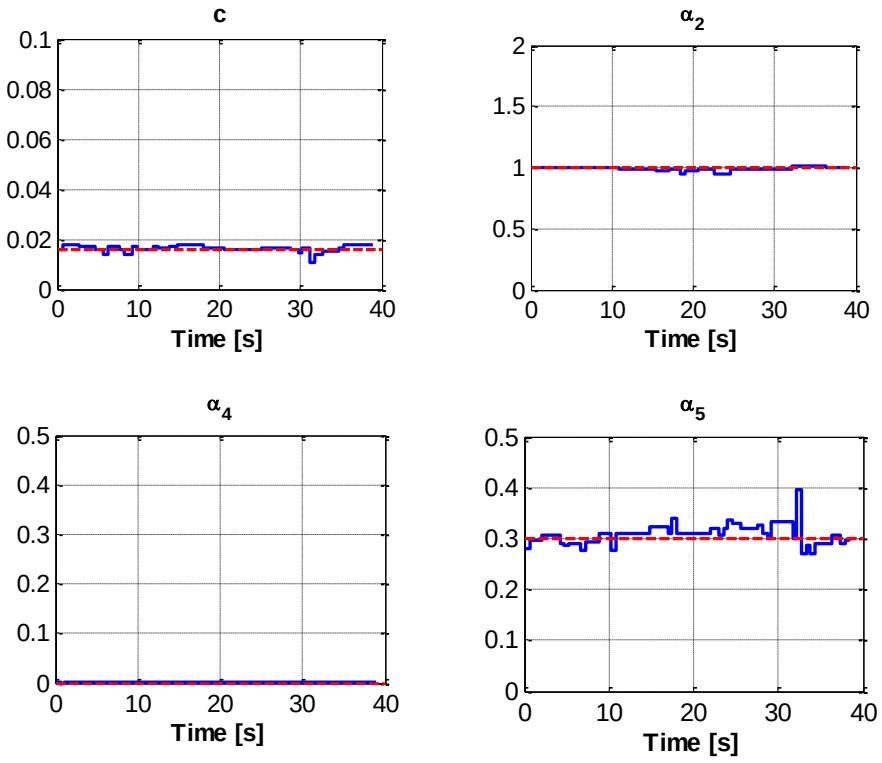

Figure 6.7 - Instantaneous coefficients identified (the straight dashed line represents the real value of the parameter): viscous damping *c*, linear stiffness α_2, α_4 term (which should be 0), nonlinear stiffness cubic term α_6

6.3.2.2.2 Example 4: Instantaneous identification of a SDoF system with Bouc-Wen hysteresis under seismic excitation

The $\dot{f}$ formulation is the most natural for the identification of hysteretic systems. In this example a Bouc-Wen model (Equation (6.46)) is identified through a XVF model. For the parameters of the Bouc-Wen model read table 6.5.

Parameter	**M [kg]**	**A [N/m]**	**β**	**γ**	**n**
Value	43000	3e6	10	5	1
Initial guess	fixed	3e6	0	0	1
Lower bound	fixed	2.5e6	0	-30	0.5
Upper bound	fixed	3.5e6	30	30	4

Table 6.5 - SDoF Bouc-Wen system parameters (the bound values refers to example 5).

"Measured" response has been obtained by numerical simulations on the Bouc-Wen model subjected to the El Centro earthquake record, with two different intensity: the 25% and the 100% of the El Centro earthquake pga, respectively. In Figure 6.9 it is possible to notice that the response produced by the lower excitation is basically linear, while, at the highest level of excitation, the loops are wider and they show a strongly nonlinear behaviour.

It is worth noting that a few polynomial terms approximating a Bouc-Wen model are directly associated to the polynomial coefficients in (6.48). For instance by comparing Equation (6.46) and (6.48) one can set $A \cong a_2$, and the following approximate relationship holds:

$$\beta|\dot{x}|\cdot|f|^n \operatorname{sgn}(f) \propto \alpha_9 \dot{x}^2 f \tag{6.49}$$

based on the fact that $|\dot{x}|$ and $\dot{x}^2$ have the same sign at every instant. Consequently, it is possible to determine the polynomial coefficient, related to the Bouc-Wen parameter β:

$$\alpha_9(t) = \frac{\beta|f|^{n-1}}{|\dot{x}|} \tag{6.50}$$

when the exponent n is equal 1, the ratio reduces to β over the modulus of the velocity. According to (6.50), the coefficient is not constant in time, especially when $\dot{x}$ is close to zero. As the spectrogram is virtually unable to provide on-line estimates, the values supplied by the estimators should be compared to the result of time-averaging on the interval ($\bar{t}$ -Δt, $\bar{t}$ +Δt), i.e. the duration of the analysis window of the spectrogram.

Similarly, for γ coefficient one has:

$$\gamma \cdot \dot{x} \cdot |f|^n \;\propto\; \alpha_{10} \cdot \dot{x} \cdot f^2 \quad \Rightarrow \quad \alpha_{10}(t) \propto \gamma |f|^{n-2} \tag{6.51}$$

Also in this case, assuming that n is equal 1, the instantaneous coefficient will be the ratio between γ and the modulus of the hysteretic force. Eqs. (6.50) and (6.51) show the dependence of the polynomial coefficients on the excitation level, as implied by the

Weierstrass approximation theorem [110]. Eqs. (6.50) and (6.51) are employed to verify the consistency of the polynomial identification.

In order to initialise the identification procedure of Equation (6.41) the values of the coefficients were all set to zero, except for the linear stiffness terms, whose starting value was supposed to be known.

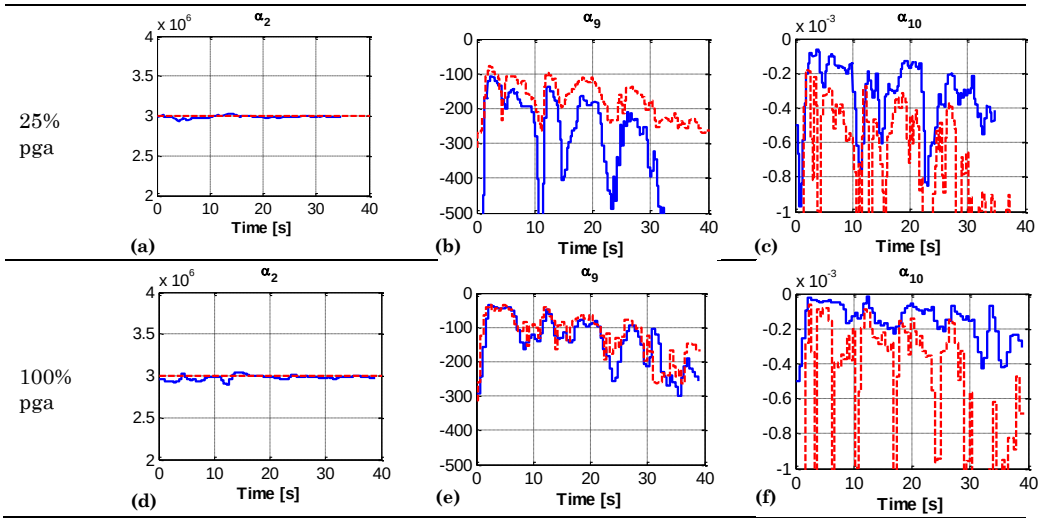

Figure 6.8 - Instantaneous coefficients identified for the 25% pga level (a)-(b)-(c) and for the 100% pga level (d)-(e)-(f) (continuous line) compared to the expected ones as defined by equations (6.50) and (6.51) (dashed line)

Figure 6.8 shows the estimated parameters for the two excitation levels; one may notice that the instantaneous coefficients matches the expected values obtained by time-averaging over the analysis window length (Equation (6.50) and (6.51)). The quality of the fitting apparently decreases with the level of excitation (Figure 6.9).

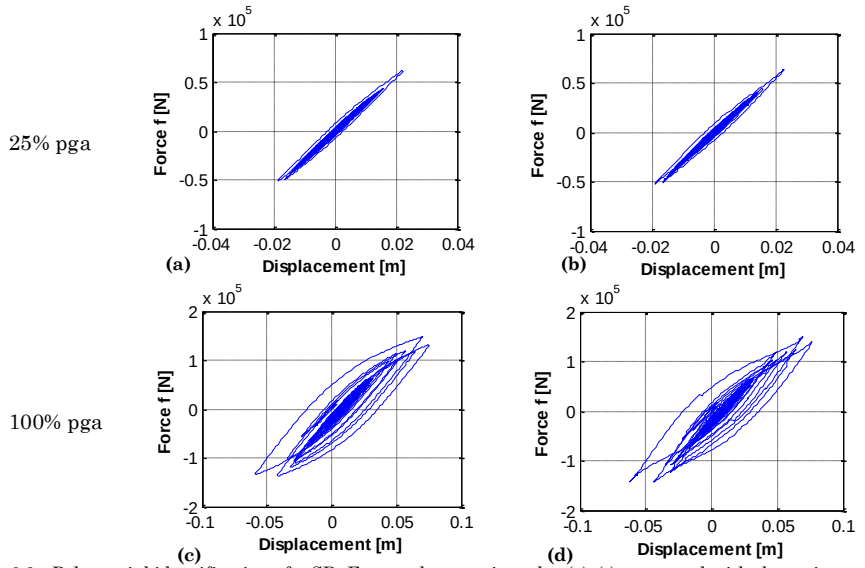

Figure 6.9 - Polynomial identification of a SDoF: exact hysteretic cycles (a)-(c) compared with the estimated ones (b)-(d) for the different excitation levels

6.3.2.2.3 Example 5: Polynomial identification of a MDoF system under earthquake excitation with different levels of noise

Identification methods must admit generalisations to multi-degrees of freedom systems, which represent a vast majority of engineering systems. In this section nonlinear identification techniques will be applied to a 2DoF system, characterised by a Bouc-Wen nonlinearity (figure 6.13 and figure 6.14). The equations of motion of the system are defined as follows:

$$\begin{cases} [M]\{\ddot{x}\}+\{f\}=-[M]\{t\}\,\ddot{x}_g(t) \\ \{\dot{f}\}=[K]\{\dot{x}\}+\{\dot{f}\}_{NL} \\ \dot{f}_{NL_1}=-|f_1+f_2|^{n_1}\left[\beta_1\cdot\mathrm{sgn}\left((f_1+f_2)\dot{x}_1\right)+\gamma_1\right]\dot{x}_1+|f_2|^{n_2}\left[\beta_2\cdot\mathrm{sgn}\left(f_2(\dot{x}_2-\dot{x}_1)\right)+\gamma_2\right](\dot{x}_2-\dot{x}_1) \\ \dot{f}_{NL_2}=-|f_2|^{n_2}\left[\beta_2\cdot\mathrm{sgn}\left(f_2(\dot{x}_2-\dot{x}_1)\right)+\gamma_2\right](\dot{x}_2-\dot{x}_1) \end{cases} \tag{6.52}$$

where [M] and [K] are the lumped mass and linear stiffness matrixes, {t} is a unitary connectivity vector and $\ddot{x}_g$ is the ground acceleration, whilst f_{NL_1} and f_{NL_2} are the nonlinear parts of the restoring forces transmitted to the first and second floor, respectively, in the assumption that they have a chain-like Bouc-Wen form.

Parameter	$\mathbf{m_1}$ **[kg]**	$\mathbf{m_2}$ **[kg]**	$\mathbf{k_{11}}$ **[N/m]**	$\mathbf{k_{12}}$ **[N/m]**	$\mathbf{k_{22}}$ **[N/m]**	$\boldsymbol{\beta_1}$	$\boldsymbol{\beta_2}$	$\boldsymbol{\gamma_1}$	$\boldsymbol{\gamma_2}$	$\mathbf{n_1}$	$\mathbf{n_2}$
Value	43000	39000	1.8e7	-8.0e6	5.5e6	15	10	2	-2	1	0.8
Initial guess	fixed	fixed	1.8e7	-8.0e6	5.5e6	0	0	0	0	1	1
Lower bound	fixed	fixed	1.62e7	-8.8e6	0.49e6	0	0	-40	-40	0.5	0.5
Upper bound	fixed	fixed	1.98e7	-7.2e6	0.61e6	40	40	40	40	4	4

Table 6.6 - Values of the parameters for the 2-DoF system (the bounds will be used in the next example 6.3.2.3.2).

The identification has been performed using the same numerical earthquakes which have been previously applied to the SDoF example, with the same pga levels. The frequencies of the underlying linear system are f_1=1.01 Hz and f_2=3.62 Hz. In order to fit a whole hysteresis loop, the length of the analysis window used in the identification process was chosen to 200 samples, which corresponds to a time length of about 2 s. This example will be recalled in the next section (6.3.2.3.2).

The polynomial approximation of the system, resorting to the XVF representation of the restoring force derivative, assumes the following form:

$$
\begin{cases}
m_1\ddot{x}_1 + f_1 = u_1(t) \\
m_2\ddot{x}_2 + f_2 = u_2(t) \\
\dot{f}_1 = \alpha_1 x_1 + \alpha_2 x_2 + \alpha_3 \dot{x}_1 + \alpha_4 \dot{x}_2 + \alpha_5 f_1 + \alpha_6 f_2 + \alpha_7 x_1 \dot{x}_1 f_1 + \alpha_8 x_2 \dot{x}_2 f_2 + \ldots \\
\ldots + \alpha_9 \cdot x_1^2 \dot{x}_1 + \alpha_{10} \cdot x_2^2 \dot{x}_2 + \alpha_{11} \cdot x_1 \dot{x}_1^2 + \alpha_{12} \cdot x_2 \dot{x}_2^2 + \alpha_{13} x_1^2 f_1 + \alpha_{14} x_2^2 f_2 \ldots \\
\ldots + \alpha_{15} x_1 f_1^2 + \alpha_{16} x_2 f_2^2 + \alpha_{17} \dot{x}_1^2 f_1 + \alpha_{18} \dot{x}_2^2 f_2 + \alpha_{19} \dot{x}_1 f_1^2 + \alpha_{20} \dot{x}_2 f_2^2 + \ldots \\
\ldots + \alpha_{21} x_1^3 + \alpha_{22} x_2^3 + \alpha_{23} \dot{x}_1^3 + \alpha_{24} \dot{x}_2^3 + \alpha_{25} f_1^3 + \alpha_{26} f_2^3 \\
\dot{f}_2 = \beta_1 x_1 + \beta_2 x_2 + \beta_3 \dot{x}_1 + \beta_4 \dot{x}_2 + \beta_5 f_1 + \beta_6 f_2 + \beta_7 x_1 \dot{x}_1 f_1 + \beta_8 x_2 \dot{x}_2 f_2 + \ldots \\
\ldots + \beta_9 \cdot x_1^2 \dot{x}_1 + \beta_{10} \cdot x_2^2 \dot{x}_2 + \beta_{11} \cdot x_1 \dot{x}_1^2 + \beta_{12} \cdot x_2 \dot{x}_2^2 + \beta_{13} x_1^2 f_1 + \beta_{14} x_2^2 f_2 \ldots \\
\ldots + \beta_{15} x_1 f_1^2 + \beta_{16} x_2 f_2^2 + \beta_{17} \dot{x}_1^2 f_1 + \beta_{18} \dot{x}_2^2 f_2 + \beta_{19} \dot{x}_1 f_1^2 + \beta_{20} \dot{x}_2 f_2^2 + \ldots \\
\ldots + \beta_{21} x_1^3 + \beta_{22} x_2^3 + \beta_{23} \dot{x}_1^3 + \beta_{24} \dot{x}_2^3 + \beta_{25} f_1^3 + \beta_{26} f_2^3
\end{cases}
\tag{6.53}
$$

In Equation (6.53) the derivatives of the restoring forces are identified through XVF polynomial models. In this example, it is deemed convenient to use 3rd order polynomial neglecting cross polynomial terms between different DoF. It is assumed that those terms are not relevant in this context.

Nonlinear terms are supposed to be unknown, while the linear stiffness is initialised to its exact value, as in the SDoF examples.

Also in this case, the XVF identified polynomial was seen to describe the system in a satisfactory manner (Figure 6.10), especially at the lower excitation level. The polynomial terms show the typical trends as in SDoF examples, those depending on the same considerations as section 6.3.2.2.2.

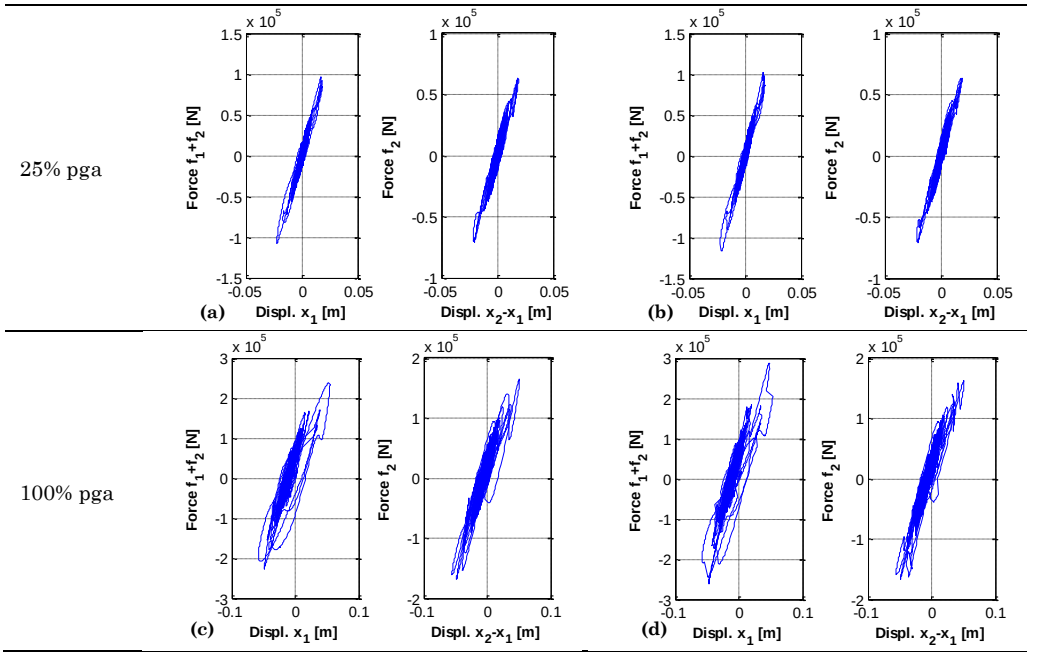

Figure 6.10 - Polynomial identification of a 2DoF system: exact hysteretic cycles (a)-(c) compared with the estimated ones (b)-(d) for the different excitation levels.

In this case both the input and the output have been contaminated in turn with three different levels of noise: zero, 2% and 5% noise. The results in table 6.7 show that the NRMS error increases with noise, but errors remain in a satisfactory range.

	Polynomial			
	25% pga		**100% pga**	
Noise	*x*	*f*	*x*	*f*
0%	0.3%	1.13%	0.5%	2.1%
2%	1.1%	1.76%	0.96%	2.3%
5%	1.5%	2.8%	1.4%	2.8%

Table 6.7 - NRMS error of displacement and hysteretic force for different noise levels: 0%, 2% and 5% SNR for the polynomial identification approach of the 2DoF hysteretic system.

6.3.2.3 Parametric identification in the time-frequency domain

When the type of model is known a priori, nonlinear instantaneous identification may identify directly the parameters of the model in question. In this case, instantaneous estimates are to be optimised so that the response, obtained by direct integration, matches experimental data. For instance, in the case of a Bouc-Wen hysteretic system, as defined by Equation (6.46), it will be possible to minimise the following vector of parameters $\mathbf{p} = \{A, \beta, \gamma, n\}$. This approach evidently lacks of generality, but, whenever applicable, is expected to be more direct and accurate [111,112].

6.3.2.3.1 Example 6: Parametric identification of an oscillator with Bouc-Wen nonlinearity under seismic excitation

In the parametric estimation of a Bouc-Wen model it is possible to introduce some constraints over the parameters. For the thermodynamic admissibility of the model and other considerations [107,109,113], the following relationships apply:

$$\begin{aligned} &A, \beta > 0 \\ &n > 0 \\ &-\beta \le \gamma \le \beta \end{aligned} \tag{6.54}$$

Moreover, the maximum value that the restoring force may assume is limited by the following relationship (for $\beta + \gamma > 0$):

$$\left| f_{\max} \right| < \sqrt[n]{\frac{A}{\beta + \gamma}} \tag{6.55}$$

Equation (6.54) and (6.55) have been used in the identification process in order to define a set of linear and nonlinear constraints, respectively, to better identify the parameters to be estimated by minimising (6.41) via a Pattern Search algorithm.

This numerical example identifies the same signals used in the example of section 6.3.2.2.2 and the parameters to be estimated were listed in table 6.5.

The initial values of the nonlinear parameters β and γ are assumed to be zero and 1 for the exponent n, whilst the linear stiffness is initialized with its correct value (see Table 6.5). As it is possible to notice from figure 6.11 with parametric identification the fitting of the time-history response and of the hysteretic cycle is improved with respect to the polynomial estimation, especially in the case of higher level of excitation. Figure 6.12 shows that estimates of the Bouc-Wen parameters become more stable at the higher excitation levels. Indeed, with lower excitations, nonlinearity is still latent. Table 6.8 shows the NRMS errors in the identification, which are seem to be smaller than 1%.

25%

100%

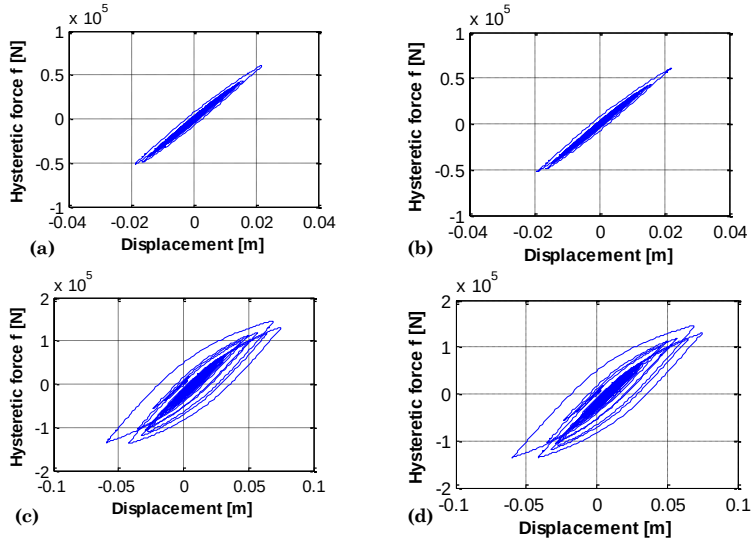

Figure 6.11 - Parametric identification of a SDoF: exact hysteretic cycles (a)-(c) compared with the estimated ones (b)-(d) for the different excitation levels

NRMS	x	$\dot{x}$	$\ddot{x}$	f
25% pga	0.67%	0.94%	1.00%	1.06%
100% pga	0.17%	0.73%	0.18%	0.25%

Table 6.8 - NRMS error of the different state variables for the Bouc-Wen identification of the SDoF hysteretic system.

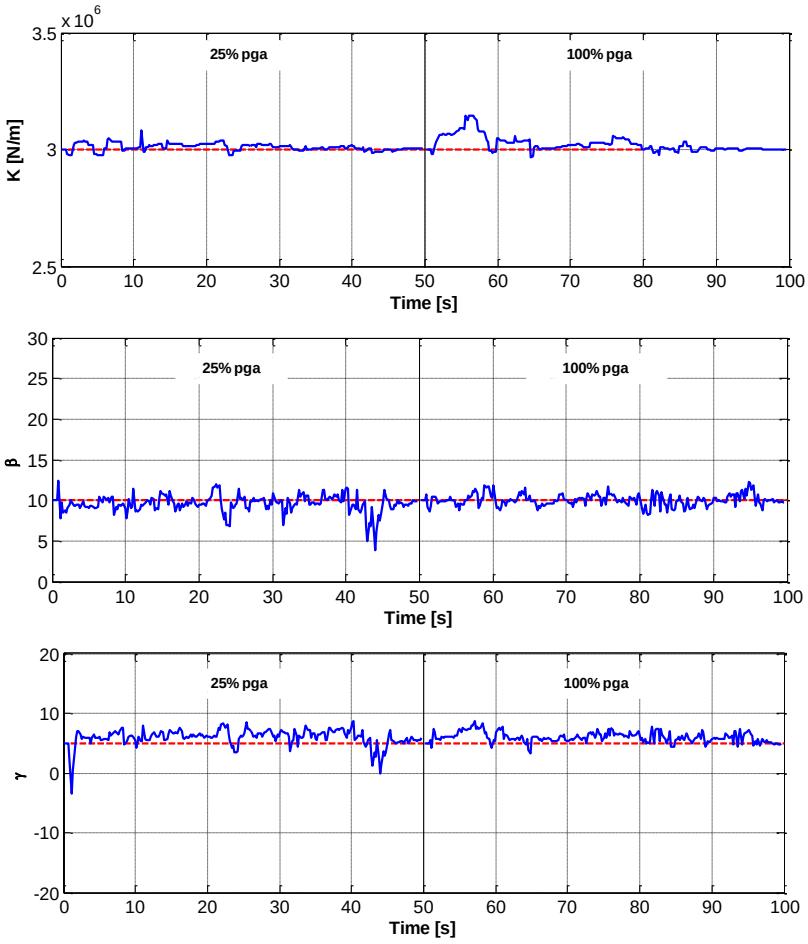
x 10^6
3.5
3
2.5
K [N/m]
25% pga
100% pga
0 10 20 30 40 50 60 70 80 90 100
Time [s]
30
25
20
15
10
5
0
β
25% pga
100% pga
0 10 20 30 40 50 60 70 80 90 100
Time [s]
20
10
0
-10
-20
γ
25% pga
100% pga
0 10 20 30 40 50 60 70 80 90 100
Time [s]

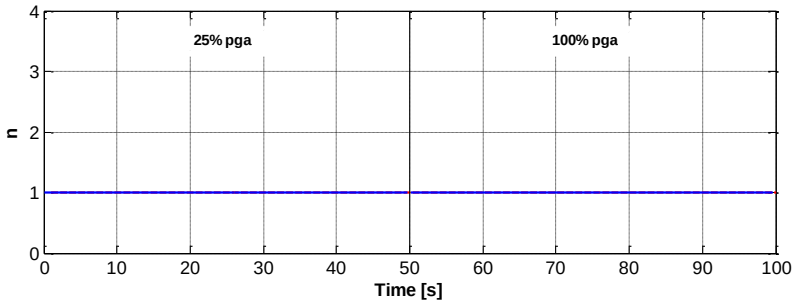

Figure 6.12 - Identified parameters of the Bouc-Wen model at different excitation levels (dashed line: identified parameters, continuous line: exact parameters)

6.3.2.3.2 Example 7: parametric identification of a 2-DoF hysteretic system under earthquake excitation

The parametric identification directly employs the response calculated through Equation (6.52). Bouc-Wen parameters to be estimated are subject to constraints, as in the SDoF case [107,109]:

$$\begin{aligned} &\beta_1, \beta_2 > 0 \\ &n_1, n_2 > 0 \\ &-\beta_1 \le \gamma_1 \le \beta_1 \quad -\beta_2 \le \gamma_2 \le \beta_2 \end{aligned} \tag{6.56}$$

Equation (6.56) has been used in the identification process in order to define a set of linear constraints for the parameters to be estimated by minimising (6.41) via a Pattern Search algorithm.

25% pga

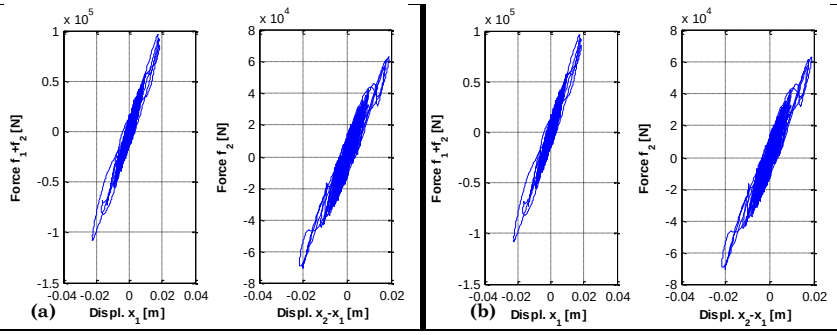

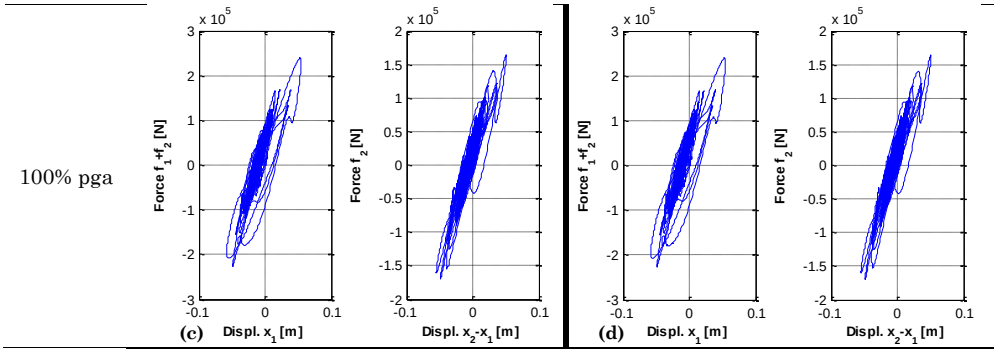

Figure 6.13 - Parametric identification of a 2DoF system: exact hysteretic cycles (a)-(c) compared with the estimated ones (b)-(d) for the different excitation levels.

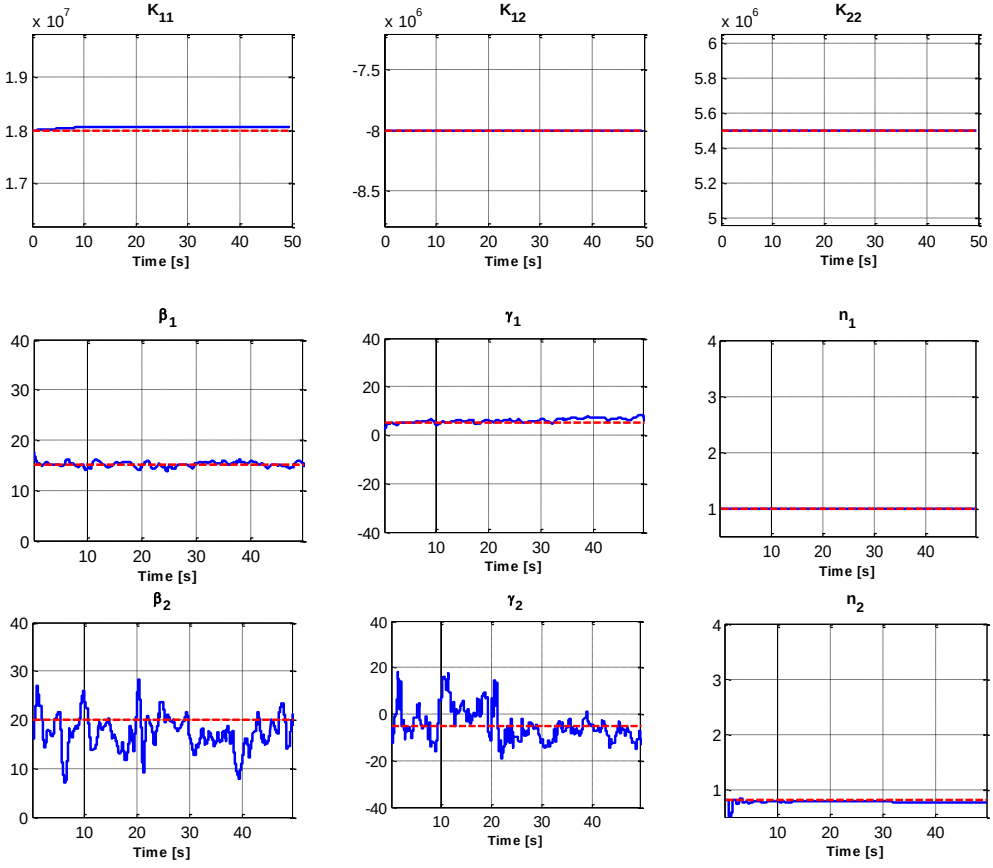

Figure 6.14 - Identified Bouc-Wen parameters at 25% pga excitation level (continuous line: identified parameters, dashed line: exact parameters)

Figure 6.13 shows the results of the parametric identification at the two different excitation levels. It is possible to notice that the two responses are virtually identical, both in terms of displacements and of hysteretic force. Figure 6.14 lists the identified parameters with the 100% pga earthquake. Nonlinear parameter estimates appear to be relatively stable and their mean value is close to the real values.

As in the polynomial identification, the identification process has also been performed in the presence of noise at 2% and 5%. As in the SDoF case, the initial value of nonlinear parameters is zero, except for the parameters n_i, which were assumed to be 1. The linear parameters are initialised with their correct values. The estimation of the parameters seems to perform better when the excitation level is higher (as already noticed in the SDoF example). The performances of the identification are satisfactory even at the higher excitation level. In this case, the quality of the fitting is very high (Table 6.9) and seems to be robust with respect to the data corruption.

	Parametric BW			
	25% pga		**100% pga**	
Noise	x	f	x	f
0%	0.03%	0.10%	0.08%	0.14%
2%	0.65%	0.91%	0.59%	0.76%
5%	1.51%	2.23%	1.38%	1.97%

Table 6.9 - NRMS error of displacement and hysteretic force for different noise levels: 0%, 2% and 5% SNR for the parametric identification approach of the 2DoF hysteretic system.

6.3.2.3.3 Example 8: parametric identification of a 2-DoF pinching-hysteretic system under earthquake excitation

In this example, a 2-DoF system with pinching is identified using the model proposed in equation (5.42). As in the previously examples, the system has been excited by the El Centro earthquake and the parameters are estimated by minimising (6.41) via a Pattern Search algorithm.

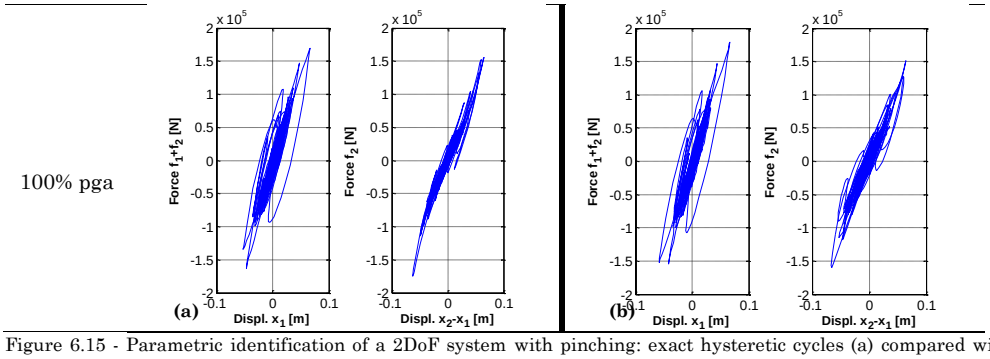

Figure 6.15 - Parametric identification of a 2DoF system with pinching: exact hysteretic cycles (a) compared with the estimated ones (b).

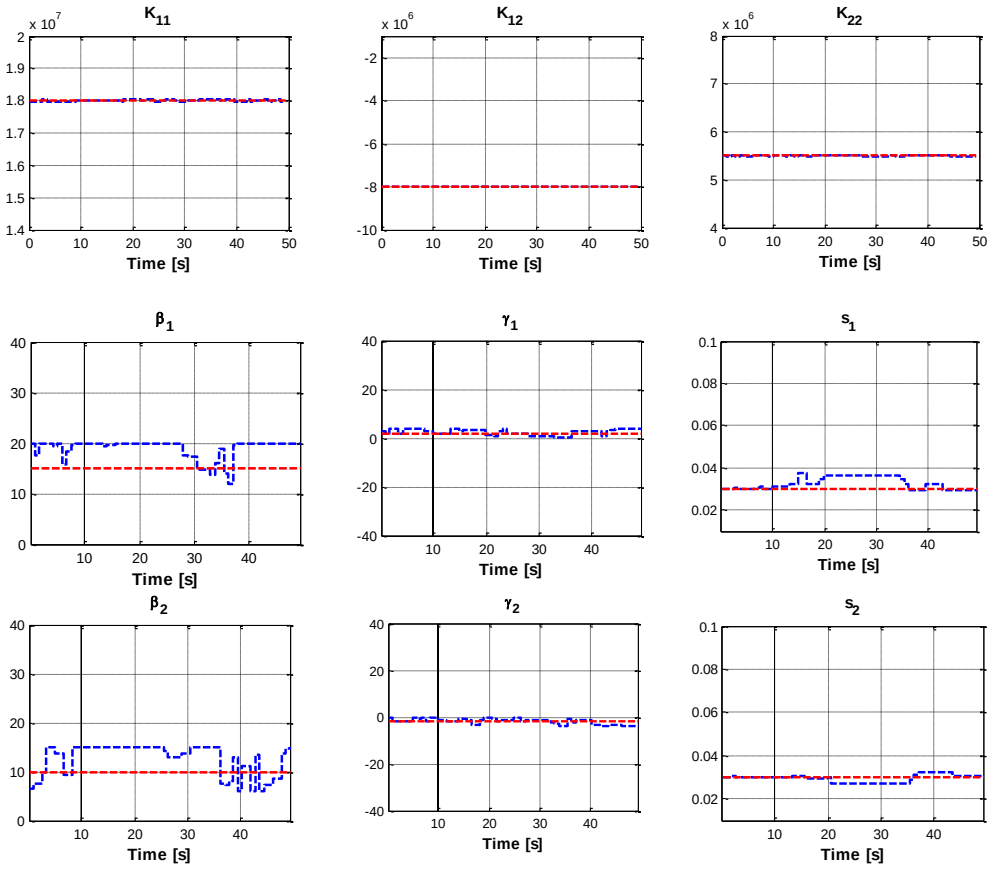

Figure 6.16 - Identified Bouc-Wen parameters at 100% pga excitation level (continuous line: identified parameters, dashed line: exact parameters)

Figure 6.16 shows the results of the parametric identification at the 100% of pga for the pinching 2-DoF system. The most significant parameters have been plotted: it is possible to notice a good agreement in terms of K, γ and s, while the parameter β shows a little bias probably due to the relatively low hysteresis of the cycles. Anyway, the quality of the identification is still reliable, in fact the normalised error in term of displacements is of the 3.20% and in term of forces is 4.67%.

6.3.3 Kalman filter and its application to nonlinear systems

The Kalman Filter [114] is a classical method applied to linear systems that have Gaussian white noise disturbances in the system states and outputs. This method allows to "clean" the process (this is where it comes from the name filter) and to determine the optimal state of the system. The Kalman Filter procedure allows also for identifying the system parameters if they are unknown. Within the nonlinear field, different extensions of the method have been proposed in the last decades.

6.3.3.1 The Extended Kalman Filter (EKF)

The first approach to parameter estimation in nonlinear field is the one proposed through the so-called Extended Kalman Filter (EKF) [115]. When working with nonlinear processes the optimality of the estimation is lost and, even worst, the estimate may diverge [116]. The EKF extends the Kalman Filter to nonlinear optimal filtering. It forms a Gaussian approximation to the joint distribution of state and measurements by resorting to a Taylor series based transformation.

In detail, it is possible to define the continuous equations of a general dynamic system by resorting to the state-space equation and it measurement equation as follows:

$$\begin{cases} \left\{\dot{X}(t)\right\} = f\left(\left\{X(t)\right\},\left\{u(t)\right\},\left\{q(t)\right\}\right) & \left\{q(t)\right\} \sim N\left(\left\{0\right\},\left[Q(t)\right]\right) \\ \left\{Y(t)\right\} = h\left(\left\{X(t)\right\},\left\{r(t)\right\}\right) & \left\{r(t)\right\} \sim N\left(\left\{0\right\},\left[R(t)\right]\right) \end{cases} \tag{6.57}$$

where $\left\{u(t)\right\}$ is the system input, $\left\{w(t)\right\}$ is the system process noise vector and $\left\{v(t)\right\}$ is the measurement noise, and $f(.)$ and $h(.)$ are nonlinear functions.

The discrete formulation of the previous equation allows applying Kalman Filtering to the system:

$$\begin{aligned} \left\{X\right\}_k &= f\left(\left\{X\right\}_{k-1},\left\{u\right\}_{k-1}\right) + \left\{q\right\}_k \\ \left\{Y\right\}_k &= h\left(\left\{X\right\}_k\right) + \left\{r\right\}_k \end{aligned} \tag{6.58}$$

The Extended Kalman Filter procedure can be initialised by defining the initial state vector $\left\{X_0\right\} = E\left[\left\{X(t_0)\right\}\right]$ and covariance matrix $\left\{P_0\right\} = Var\left[\left\{X(t_0)\right\}\right]$. Like all the algortihms based on Kalman Filter, the EKF algorithm involves two basic steps in the estimation process: a prediction phase, where the next state of the system is predicted given the previous measurements, and an updating phase, where the current state of the system is estimated given the measurement at that time step.

For what concerns the prediction phase, a guess of the state vector based on the system state can be done as follows:

$$\begin{cases} \{X\}_k^- = f\left(\{X\}_{k-1},\{u\}_{k-1}\right) \\ \left[P\right]_k^- = F_X\left(\{X\}_{k-1},\{u\}_{k-1}\right)\left[P\right]_{k-1}F_X^T\left(\{X\}_{k-1},\{u\}_{k-1}\right)+\left[R\right]_k \end{cases} \tag{6.59}$$

Where F_X and H_X are the Jacobians of f and h, defined as follows:

$$\begin{aligned} \left[F_X\left(\{X\}_{k-1},\{u\}_{k-1}\right)\right]_{j,j'} &= \frac{\partial f_j\left(\{X\}_{k-1},\{u\}_{k-1}\right)}{\partial x_{j'}} \\ \left[H_X\left(\{X\}_k\right)\right]_{j,j'} &= \frac{\partial h_j\left(\{X\}_k\right)}{\partial x_{j'}} \end{aligned} \tag{6.60}$$

The updating step involves the definition of optimal Kalman gain, and may be defined as follows:

$$\begin{cases} \left[K\right]_k = \left[P\right]_k^- \cdot H_X^T\left(\{X\}_k\right)\cdot\left(H_X\left(\{X\}_k\right)\cdot\left[P\right]_k^- \cdot H_X^T\left(\{X\}_k\right)+\left[R\right]_k\right)^{-1} \\ \left\{\hat{X}\right\}_k = \left\{\hat{X}\right\}_k^- + \left[K\right]_k\left(\{Y\}_k - h\left(\left\{\hat{X}\right\}_k^-\right)\right) \\ \left[P\right]_k = \left[P\right]_k^- - \left[K\right]_k\left(H_X\left(\{X\}_k\right)\cdot\left[P\right]_k^- \cdot H_X^T\left(\{X\}_k\right)+\left[R\right]_k\right)\left[K\right]_k^T \end{cases} \tag{6.61}$$

The EKF has some flaws: as previously mentioned, the EKF is not an optimal estimator; moreover if the initial estimate of the state vector is wrong, or the process is modelled incorrectly the filter may diverge due to its linearization approach. Furthermore the estimated covariance matrix in the EKF tends to underestimate the true covariance matrix so that it risks becoming inconsistent in the statistical sense without the addition of a "stabilising noise".

6.3.3.2 The Unscented Kalman Filter (UKF)

The Unscented Kalman Filter (UKF) is a recently proposed technique (see for reference [117,118]) which has the advantage with respect to the canonical EKF of being able to handle any type of nonlinearity. In detail, UKF does not require the computation of the Jacobian of the nonlinear function; in fact it does not approximate the measurement equation of the system but it approximates the posterior probability density by a Gaussian density, by using a set of deterministic points (the so-called Sigma points). When the Sigma points are propagated through the nonlinear transform, they capture the true mean and covariance of the Gaussian random variables, and the posterior mean and covariance accurately to the 3rd order Taylor series expansion for any nonlinearity.

Starting from the discrete equations for a dynamic system (6.58), one can define the augmented state vector as:

$$\{X\}_{k-1}^{a} = \left[\{X\}_{k-1}^{T} \; [q]_{k-1} \; \{r\}_{k-1} \right] \tag{6.62}$$

which can be initialised as follows:

$$\left\{\hat{X}\right\}_{0}^{a} = E\left[\{X\}^{a}\right] = \left[\left\{\hat{X}\right\}_{0}^{T} \quad \{0\} \quad \{0\} \right] \tag{6.63}$$

Accordingly, it is possible to define an augmented covariance matrix and initialise it:

$$[P]_{0}^{a} = E\left[\left(\{X\}_{0}^{a} - \left\{\hat{X}\right\}_{0}^{a} \right) \left(\{X\}_{0}^{a} - \left\{\hat{X}\right\}_{0}^{a} \right)^{T} \right] \tag{6.64}$$

Successively, one can compute a deterministic set of sample points (or Sigma points), with associated weights:

$$\{\mathcal{X}\}_{k-1}^{a} = \left[\left\{\hat{X}\right\}_{k-1}^{a} \quad \left\{\hat{X}\right\}_{k-1}^{a} + \sqrt{(L+\lambda)[P]_{k-1}^{a}} \quad \left\{\hat{X}\right\}_{k-1}^{a} - \sqrt{(L+\lambda)[P]_{k-1}^{a}} \right] \tag{6.65}$$

where L is the dimension of the augmented state vector and λ is a scale factor (for an extensive discussion on this, see [119,120]). Once the sigma points $\{\mathcal{X}\}_{k-1}^{a}$ are computed it is possible to determine the predicted state vector $\left\{\hat{X}\right\}_{k}^{-}$ and the predicted covariance $\left[\hat{P}\right]_{k}^{-}$ by propagating the sigma points as follows:

$$\begin{aligned}
\{\mathrm{X}\}_{k}^{\{X\}} &= f\left(\{\mathrm{X}\}_{k-1}^{\{X\}}, \{u\}_{k-1}, \{\mathrm{X}\}_{k-1}^{\{q\}} \right) \\
\left\{\hat{X}\right\}_{k}^{-} &= \sum_{i=0}^{2L} W_i^{(m)} \{\mathrm{X}\}_{i,k}^{\{X\}} \\
[P]_{k}^{-} &= \sum_{i=0}^{2L} W_i^{(c)} \left[\{\mathrm{X}\}_{i,k}^{\{X\}} - \left\{\hat{X}\right\}_{k}^{-} \right] \left[\{\mathrm{X}\}_{i,k}^{\{X\}} - \left\{\hat{X}\right\}_{k}^{-} \right]^{T}
\end{aligned} \tag{6.66}$$

The values of the weights for the mean ($W_i^{(m)}$) and for the covariance ($W_i^{(c)}$) can be computed as reported in [119]. Once the predicted values are computed, one has to compute the predicted measurement vector by using the Sigma point approximation:

$$
\begin{aligned}
&\{\mathrm{Y}\}_{k}^{\{X\}} = h\left(\{\mathrm{X}\}_{k}^{\{X\}}, \{\mathrm{X}\}_{k}^{\{q\}}\right) \\
&\left\{\hat{Y}\right\}_{k}^{-} = \sum_{i=0}^{2L} W_i^{(m)} \{\mathrm{Y}\}_{i,k}^{\{X\}} \\
&\left[P\right]_{k}^{YY} = \sum_{i=0}^{2L} W_i^{(c)} \left[\{\mathrm{Y}\}_{i,k}^{\{X\}} - \left\{\hat{Y}\right\}_{k}^{-}\right]\left[\{\mathrm{Y}\}_{i,k}^{\{X\}} - \left\{\hat{Y}\right\}_{k}^{-}\right]^{T}
\end{aligned}
\tag{6.67}
$$

The measurement update can be performed as follows:

$$
\begin{aligned}
&\left[P\right]_{k}^{XY} = \sum_{i=0}^{2L} W_i^{(c)} \left[\{\mathrm{X}\}_{i,k}^{\{X\}} - \left\{\hat{X}\right\}_{k}^{-}\right]\left[\{\mathrm{Y}\}_{i,k}^{\{X\}} - \left\{\hat{Y}\right\}_{k}^{-}\right]^{T} \\
&\left[\mathrm{K}\right]_{k} = \left[P\right]_{k}^{XY}\left(\left[P\right]_{k}^{YY}\right)^{-1} \\
&\left\{\hat{X}\right\}_{k} = \left\{\hat{X}\right\}_{k}^{-} + \left[\mathrm{K}\right]_{k}\left(\{Y\}_{k} - \left\{\hat{Y}\right\}_{k}^{-}\right) \\
&\left[P\right]_{k} = \left[P\right]_{k}^{-} - \left[\mathrm{K}\right]_{k}\left[P\right]_{k}^{YY}\left[\mathrm{K}\right]_{k}^{T}
\end{aligned}
\tag{6.68}
$$

The main step of the UKF is the unscented transformation described in equation (6.65) which uses a set of deterministically chosen sigma points to parametrize the mean and covariance of the probability distribution. The statistic of the propagated points is then calculated to form an estimate of the nonlinearly transformed mean and covariance. As previously stated, it is possible to notice from above that the UKF does not require the calculation of any Jacobian for linearizing the system and measurement equations. Therefore, the UKF can be used also in the case of system equations which are not differentiable (such as in the case of most hysteretic models). The UKF has been successfully applied for real-time estimation of hysteretic degrading systems with pinching in [74].

6.3.3.2.1 Example 9: Parametric identification of an oscillator with Bouc-Wen nonlinearity under seismic excitation

In order to apply the UKF, the example number 4 is presented again hereinafter. In this case the Bouc-Wen model (Equation (6.46)) is identified by defining the state vector $\{X\}$ as follows:

$$
\{X\} = \left[x_1, x_2, x_3, x_4, x_5, x_6, x_7\right] = \left[x, \dot{x}, f, A, \beta, \gamma, n\right] \tag{6.69}
$$

$$f\left(\{X\},\{u\}\right)=\begin{bmatrix} \dot{x} \\ -\frac{1}{m}\left(c\dot{x}+f\right)-u \\ \left[A-\left(\beta\cdot\mathrm{sgn}\left(\dot{x}\cdot f\right)+\gamma\right)\left|f\right|^{n}\right]\dot{x} \\ 0 \\ 0 \\ 0 \\ 0 \end{bmatrix} \tag{6.70}$$

The UKF allows performing an online identification of the hysteresis parameters reported in table 6.10. Notice that the initial guess of the parameters must be not-zero in order to avoid computational problems. At the second excitation level (100% pga) the parameter are initialised by using the identified values at the lower excitation level.

Parameter	M [kg]	A [N/m]	β	γ	n
Value	43000	3e6	10	5	1
Initial guess	fixed	3e6	1	1	1

Table 6.10 - SDoF Bouc-Wen system parameters and initial guesses in the identification process.

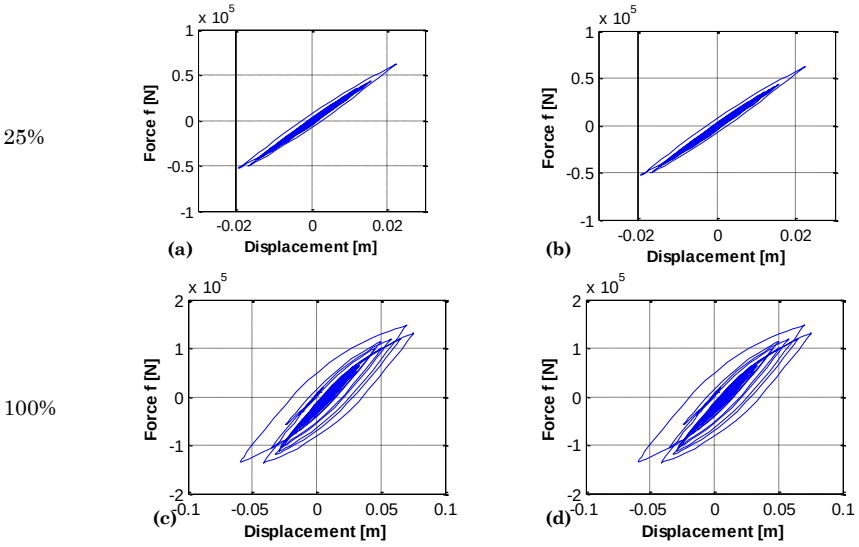

Figure 6.17 - Identification of a SDoF with UKF: exact hysteretic cycles (a)-(c) compared with the estimated ones (b)-(d) for the different excitation levels

It is possible to notice from figure 6.18 the good match between identified values and real values of the parameters, even better than in the previous example TF identification. Anyway, UKF seems to have problem when the number of parameters to be identified increase significantly (for instance, in the MDoF examples proposed before).

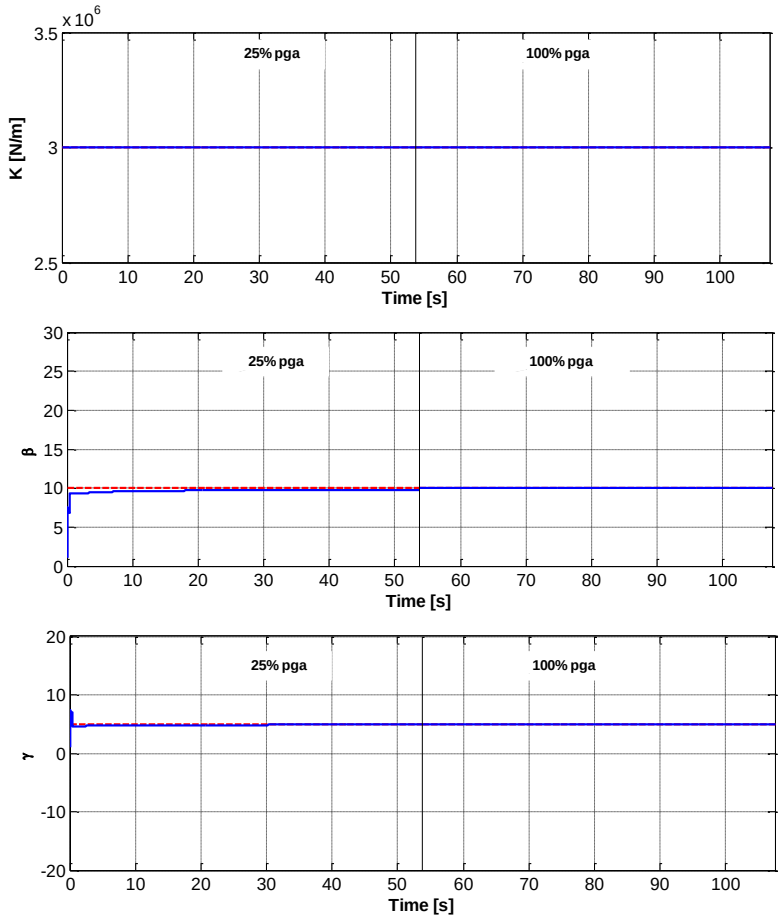
x 10^6
3.5
3
2.5
K [N/m]
25% pga
100% pga
0 10 20 30 40 50 60 70 80 90 100
Time [s]
30
25
20
15
10
5
0
β
25% pga
100% pga
0 10 20 30 40 50 60 70 80 90 100
Time [s]
20
10
0
-10
-20
γ
25% pga
100% pga
0 10 20 30 40 50 60 70 80 90 100
Time [s]

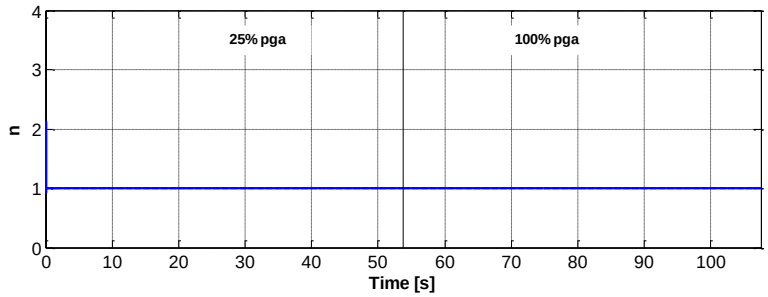

Figure 6.18 - Identified parameters of the Bouc-Wen model at different excitation levels (dashed line: identified parameters, continuous line: exact parameters).

6.3.3.3 The Iterated Unscented Kalman Filter (UKF)

A further improvement to the UKF algorithm was firstly proposed in [121] with the name of Iterated Unscented Kalman Filter (IUKF). The idea is that improved performance may be expected if iterations are to be implemented in the UKF algorithm. The steps of the IUKF can be summarised as:

- For each instant $k \geq 1$ one can evaluate the estimate $\left\{\hat{X}\right\}_k$ and the corresponding covariance matrix $\left[P\right]_k$ through equations (6.66)-(6.68).
- Let $\left\{\hat{X}\right\}_{k,0} = \left\{\hat{X}\right\}_k^-$, $\left[P\right]_{k,0} = \left[P\right]_k^-$ and $\left\{\hat{X}\right\}_{k,1} = \left\{\hat{X}\right\}_k$, $\left[P\right]_{k,1} = \left[P\right]_k$ and get iteration index j=2 and g=1.
- Generate new sigma points in the same way as (6.65):

$$\left\{\mathcal{X}\right\}_j^a = \left[\left\{\hat{X}\right\}_{k,j-1}^a \quad \left\{\hat{X}\right\}_{k,j-1}^a + \sqrt{(L+\lambda)\left[P\right]_{k,j-1}^a} \quad \left\{\hat{X}\right\}_{k,j-1}^a - \sqrt{(L+\lambda)\left[P\right]_{k,j-1}^a}\right] \tag{6.71}$$

- Recalculate all the previous steps in (6.66)-(6.68):

$$\left\{\hat{X}\right\}_{k,j}^{-}=\sum_{i=0}^{2L}W_i^{(m)}\left\{\mathrm{X}\right\}_{i,j}^{\{X\}}$$

$$\left\{\mathrm{Y}\right\}_{j}=h\left(\left\{\mathrm{X}\right\}_{j}\right)$$

$$\left\{\hat{Y}\right\}_{k,j}^{-}=\sum_{i=0}^{2L}W_i^{(m)}\left\{\mathrm{Y}\right\}_{i,j}$$

$$\left[P\right]_{k,j}^{YY}=\sum_{i=0}^{2L}W_i^{(c)}\left[\left\{Y\right\}_{i,j}-\left\{\hat{Y}\right\}_{k,j}^{-}\right]\left[\left\{Y\right\}_{i,j}-\left\{\hat{Y}\right\}_{k,j}^{-}\right]^{T}$$

$$\left[P\right]_{k,j}^{XY}=\sum_{i=0}^{2L}W_i^{(c)}\left[\left\{X\right\}_{i,j}-\left\{\hat{X}\right\}_{k,j}^{-}\right]\left[\left\{Y\right\}_{i,j}-\left\{\hat{Y}\right\}_{k,j}^{-}\right]^{T}$$

$$\left[\mathrm{K}\right]_{k,j}=\left[P\right]_{k,j}^{XY}\left(\left[P\right]_{k,j}^{YY}\right)^{-1}$$

$$\left\{\hat{X}\right\}_{k,j}=\left\{\hat{X}\right\}_{k,j}^{-}+g\left[\mathrm{K}\right]_{k,j}\left(\left\{\hat{Y}\right\}_{k}-\left\{\hat{Y}\right\}_{k,j}^{-}\right)$$

$$\left[P\right]_{k,j}=\left[P\right]_{k,j-1}-\left[\mathrm{K}\right]_{k,j}\left[P\right]_{k,j}^{YY}\left[\mathrm{K}\right]_{k,j}^{T} \tag{6.72}$$

where the subscript j denotes the j[th] iteration, $\left\{Y\right\}_{i,j}$ represents the i[th] component of $\left\{Y\right\}_{j}$.

- One can define the following three equations: $\left\{\hat{Y}\right\}_{k,j}=h\left(\left\{\hat{X}\right\}_{k,j}\right)$, $\left\{\tilde{X}\right\}_{k,j}=\left\{\hat{X}\right\}_{k,j}-\left\{\hat{X}\right\}_{k,j-1}$ and $\left\{\hat{Y}\right\}_{k,j}=\left\{Y\right\}_{k}-\left\{\hat{Y}\right\}_{k,j}$.
- If the following inequality holds:

$$\left\{\tilde{X}\right\}_{k,j}^{T}\left[P\right]_{k,j-1}^{-T}\left\{\tilde{X}\right\}_{k,j}+\left\{\tilde{Y}\right\}_{k,j}^{T}\left[R\right]_{k}^{-1}\left\{\tilde{Y}\right\}_{k,j}<\left\{\tilde{Y}\right\}_{k,j-1}^{T}\left[R\right]_{k}^{-1}\left\{\tilde{Y}\right\}_{k,j-1} \tag{6.73}$$

  and j≤N (maximum number of iteration allowed), then one has to set g=ηg (with η being a decaying factor chosen between 0 and 1), j=j+1 and return to the generation of sigma points, otherwise it is possible to exit from the iterative process and to perform the last step.
- If the inequality is not satisfied or if j is too large the procedure stops and one obtains: $\left\{\hat{X}\right\}_{k}=\left\{\hat{X}\right\}_{k,j}$ and $\left[P\right]_{k}=\left[P\right]_{k,j}$.

With respect to the standard UKF, the IUKF can adjust the state estimate to adaptively approach the true value through corrections of the measurements, so after the iterative process terminates, a lower state of error can be expected. Moreover, this

filter can respond to new measurements as quickly as possible with the adjustment of state and covariance matrix, making a faster convergence speed possible in situations where the initial error is large. This method has been successfully applied to hysteretic SDoF systems and to a 2DoF system with polynomial nonlinearity in [91] by Xie and Feng.

References

[1] Worden, K., Tomlinson, G.R., (2001); *Nonlinearity in structural dynamics: detection, identification, and modelling*, Institute of Phsysics Publishing.

[2] Adams, D.E., Allemang, R.J., (1998); *Survey of nonlinear detection and identification techniques for experimental vibrations*. Proceedings of the International Conference on Noise and Vibration Engineering, pp. 269-281.

[3] Kerschen, G., Worden, K., Vakakis, A.F., Golinval, J.C., (2006); *Past, present and future of nonlinear system identification in structural dynamics*. Mechanical Systems and Signal Processing, 20, pp. 505-592.

[4] Sracic, M.W., Allen, M.S., (2011); *Method for identifying models of nonlinear systems using linear time periodic approximations*. Mechanical Systems and Signal Processing, doi: 10.1016/j.ymssp.2011.03.004.

[5] Caughey, T.K., (1963); *Equivalent linearisation techniques*. Journal of the Acoustical Society of America, 35, pp. 1703-1711.

[6] Kazakov, I.E., (1956); *Approximate probabilistic analysis of the accuracy of operation of essentially nonlinear systems*. Automatika i Telemekhanika, 17, pp. 423-450.

[7] Ozer, M.E., Ozguven, H.N., Royston, T.J., (2005); *Identification of structural non-linearities using describing functions and Sherman-Morrison method*. Proceedings of the 23rd International Modal Analysis Conference, Orlando.

[8] Hagedorn, P., Wallaschek, J., (1987); *On equivalent harmonic and stochastic linearization*. Proceedings of the IUTAM Symposium on Nonlinear Stochastic Dynamic Engineering Systems, pp. 23-32.

[9] Mohammad, K.S., Worden, K., Tomlinson, G.R., (1992); *Direct Parameter Estimation for LInear and Non-Linear Structures*. Journal of Sound and Vibration, 152(3), pp. 471-499.

[10] Gifford, S.J., Tomlinson, G.R., (1989); *Recent advances in the applications of functional series to non-linear structures*. Journal of Sound and Vibration, 135, pp. 289-317.

[11] Masri, S.F., Caughey, T.K., (1979); *A nonparametric identification technique for nonlinear dynamic problems*. Journal of Applied Mechanics, 46, pp. 433-447.

[12] Masri, S.F., Sassi, H., Caughey, T.K., (1982); *Identification and modeling of nonlinear systems*. Nuclear Engineering and Design, 72, pp. 235-270.

[13] Crawley, E.F., Aubert, A.C., (1986); *Identification of nonlinear structural elements by force-state mapping*. AIAA Journal, pp. 155-162.

[14] Crawley, E.F., O'Donnell, K.J., (1986); *Identification of nonlinear system parameters*

in joints using the force-state mapping technique. AIAA Paper, 86, pp. 659-667.

[15] Duym, S., Schoukens, J., Guillaume, P., (1996); *A local restoring force surface method*. International Journal of Analytical and Experimental Modal Analysis, 11, pp. 116-132.

[16] Al-Hadid, M.A., Wright, J.R., (1989); *Developments in the force-state mapping technique for non-linear systems and the extension to the location of non-linear elements in a lumped-parameter system*. Mechanical Systems and Signal Processing, 3, pp. 269-290.

[17] Worden, K., Tomlinson, G.R., (1989); *Application of the restoring force method to nonlinear elements*. Proceedings of the Seventh International Modal Analysis Conference, Las Vegas.

[18] Worden, K., (1990); *Data processing and experiment design for the restoring force surface method, Part I: integration and differentiation of measured time data*. Mechanical Systems and Signal Processing, 4, pp. 295-319.

[19] Worden, K., (1990); *Data processing and experiment design for the restoring force surface method, Part II: choice of excitation signal*. Mechanical Systems and Signal Processing, 4, pp. 321-344.

[20] Benedettini, F., Capecchi, D., Vestroni, F., (1995); *Identification of Hysteretic Oscillators under earthqauke loading by Nonparameteric models*. ASCE Journal of Engineering Mechanics, pp. 606-612.

[21] Lo, H.R., Hammond, J.K., (1988); *Identification of a class of nonlinear systems*. Institute of Sound and Vibration Research.

[22] Yar, M., Hammond, J.K., (1987); *Parameter estimation for hysteretic systems*. Journal of Sound and Vibration, 117, pp. 161-172.

[23] Masri, S.F., Caffrey, J.P., Caughey, T.K., Smyth, A.W., Chassiakos, A.G., (2004); *Identification of the state equation in complex non-linear systems*. International Journal of Non-Linear Mechanics, 39, pp. 1111-1127.

[24] Visintin, A., (1994); *Differential models of hysteresis*, Springer.

[25] Masri, S.F., Miller, R.K., Saud, A.F., Caughey, T.K., (1987); *Identification of nonlinear vibrating structures: part I - formalism*. Journal of Applied Mechanics, 54, pp. 918-922.

[26] Leontaritis, I.J., Billings, S.A., (1985); *Input-output parametric models for non-linear systems, part I*. International Journal of Control, 41, pp. 329-344.

[27] Leontaritis, I.J..B.S.A., (1985); *Input-output parametric models for non-linear systems, part II*. International Journal of Control, 41, pp. 329-344.

[28] Chen, S., Billings, S.A., (1989); *Representation of non-linear systems: the NARMAX model*. International Journal of Control, 49, pp. 1013-1032.

[29] Billings, S.A., Chen, S., (1989); *Extended model set, global data and threshold model identification for severely non-linear systems*. International Journal of Control, 50, pp. 1897-1923.

[30] Korenberg, M., Billings, S.A., Liu, Y.P., (1988); *An orthogonal parameter estimation algorithm for nonlinear stochastic systems*. International Journal of Control, 48, pp.

193-210.

[31] Tao, Q.H., (1992); *Modelling and prediction of non-linear time-series*. Department of Automatic Control and System Engineering, University of Sheffield, Sheffield PhD Thesis.

[32] Bendat, J.S., (1990); *Nonlinear System Analysis and Identification from Random Data*, New York Wiley.

[33] Richards, C.M., Singh, R., (2000); *Comparison of two non-linear system identification approaches derived from "reverse path" spectral analysis*. Journal of Sound and Vibration, 237, pp. 361-376.

[34] Bendat, J.S., Coppolino, R.N., Palo, P.A., (1995); *Identification of physical parameters with memory in non-linear sistems*. International Journal of Nonlinear Mechanics, 30, pp. 841-860.

[35] Marchesiello, S., Garibaldi, L., Wright, J.R., Cooper, J.E., (2000); *Application of the Conditioned Reverse Path Method to structures with different types of non-linearities*. ISMA 25 Conference, Leuven.

[36] Garibaldi, L., Marchesiello, S., (2002); *Application of Frequency Domain Identification Method to Nonlinear Systems*. ISMA International Conference on Noise and Vibration Engineering, Leuven, Belgium, pp. 1159-1168.

[37] Kerschen, G., Golinval, J.-C., (2002); *Frequency Domain Approaches for the Identification of an Experimental Beam with a Local Non-linearity*. Proceedings of IMAC XX, Los Angeles.

[38] Marchesiello, S., (2003); *Application of the Conditioned Reverse Path Method*. Mechanical Systems and Signal Processing, 17, pp. 183-188.

[39] Adams, D.E., Allemang, R.J., (1999); *A new derivation of the frequency response function matrix for vibrating non-linear systems*. Journal of Sound and Vibration, 227(5), pp. 1083-1108.

[40] Adams, D.E., Allemang, R.J., (1999); *Characterization of Nonlinear Vibrating Systems Using Internal Feedback and Frequency Response Modulation*. ASME Journal of Vibration and Acoustics , 121(4), pp. 495-500.

[41] Adams, D.E., Allemang, R.J., (2000); *A frequency domain method for estimating the parameters of a non-linear structural dynamic model through feedback*. Mechanical Systems and Signal Processing, 14(4), pp. 637-656.

[42] Volterra, V., (1959); *Theory of Functionals and Integral Equations*, New York Dover Publications.

[43] Schetzen, M., (1980); *The Volterra and Wiener Theories of Non-Linear Systems*, New York Wiley.

[44] Worden, K., Manson, G., (1998); *Random vibrations of a duffing oscillator using the Volterra series*. Journal of Sound and Vibration, 217, pp. 781-789.

[45] Worden, K., Manson, G., (1999); *Random vibrations of a multi-degree-of-freedom non-linear system using the Volterra series*. Journal of Sound and Vibration, 226, pp. 397-405.

[46] Vazquez Feijoo, J.A., Worden, K., Stanway, R., (2002); *Identification of MDOF*

Nonlinear Systems using Associated Linear Equations (ALEs), par1: obtaining the ALEs froma MDOF Continous Nonliear System. Proceeding of ISMA 2002, pp. 1313-1221.

[47] Vazquez Feijoo, J.A., Worden, K., Stanway, R., (2005); *Associated Linear Equations for Volterra operators*. Mechanical Systems and Signal Processing, 19, pp. 57-69.

[48] Vazquez Feijoo, J.A., Worden, K., Montes Garcia, P., Lagunez Rivera, L., Juarez Rodriguez, N. et al., (2010); *Analysis of MDOF nonlinear systems using associated linear equations*. Mechanical Systems and Signal Processing, 24, pp. 2824-2843.

[49] Demarie, G.V., Ceravolo, R., De Stefano, A., (2005); *Instantaneous identification of polynomial nonlinearity based on Volterra series representation*. Key Engineering Materials, 293-294, pp. 703-710.

[50] Demarie, G.V., (2005); *Identificazione nonlineare basata su serie di Volterra*. Politecnico di Torino, PhD Thesis.

[51] McClelland, J.L., Rumelhart, D.E., (1988); *Exploration in Parallel Distributed Processing*, Cambridge MA MIT Press.

[52] Chen, S., Billings, S.A., Grant, P.M., (1990); *Non-linear system identification using neural networks*. International Journal of Control, 51, pp. 1191-1214.

[53] Masri, S.F., Chassiakos, A.G., Caughey, T.K., (1993); *Identification of nonlinear vibrating structures*. ASME Journal of Applied Mechanics, 60, pp. 123-133.

[54] Billings, S.A., Jamaluddin, H.B., Chen, S., (1991); *A comparison of the backpropagation and recursive prediction error algorithms for training neural networks*. Mechanical Systems and Signal Processing, 5, pp. 233-255.

[55] Billings, S.A., Jamaluddin, H.B., Chen, S., (1991); *Properties of neural networks with application to modelling non-linear dynamical systems*. International Journal of Control, 55, pp. 193-224.

[56] Wray, J., Green, G.G.R., (1994); *Calculation of the Volterra kernels of nonlinear dynamic systems using an artificial neural network*. Biol. Cybernet., 71, pp. 187-195.

[57] Ceravolo, R., (1995); *Metodi dinamici avanzati in diagnostica strutturale*. Politecnico di Torino, Department of Structural and Geotechnical Engineering, PhD Thesis.

[58] Priestley, M.B., (1967); *Power spectral analysis of non-stationary random processes*. Journal of Sound and Vibration, 6(1), pp. 86-97.

[59] Hammond, J.K., White, P.R., (1996); *The analysis of non-stationary signals using time-frequency methods*. Journal of Sound and Vibration, 190(3), pp. 419-447.

[60] Hammond, J.K., Waters, T.P., (2001); *Signal processing for experimental modal analysis*. Philosophical Transactions of the Royal Society A, 359(1778), pp. 41-59.

[61] Ceravolo, R., (2009); Time-frequency analysis, in: Boller, C., Chang, F.K., Fujino, Y., *Encyclopedia of Structural Health Monitoring*, Chirchester, UK, Wiley & Sons Ltd, ch. 26.

[62] Feldman, M., (2008); *Theoretical analysis and comparison of the Hilbert transform decomposition methods*. Mechanical Systems and Signal Processing, 22(3), pp. 509-519.

[63] Huang, N.E., Shen, Z., Long, S.R., Wu, M.C., Shih, H.H. et al., (1998); *The Empirical*

Mode Decomposition and the Hilbert spectrum for nonlinear and non-stationary Time Series Analysis. Proceedings: Mathematical, Physical and Engineering Sciences, 454(1971), pp. 903-995.

[64] Yang, J.N., Lei, Y., Pan, S., Huang, N., (2003); *System identification of linear structures based on Hilbert–Huang spectral analysis. Part I: Normal Modes*. Earthquake Engineering & Structural Dynamics, 32, pp. 1443-1467.

[65] Yang, J.N., Lei, Y., Pan, S., Huang, N., (2003); *System identification of linear structures based on Hilbert–Huang spectral analysis. Part II: Complex Modes*. Earthquake Engineering & Structural Dynamics, 32, pp. 1533-1554.

[66] Yang, J.N., Lei, Y., Lin, S., Huang, N., (2004); *Hilbert-Huang based approach for structural damage detection*. ASCE Journal of Engineering Mechanics, 130(1), pp. 85-95.

[67] Spina, D., Valente, C., Tomlinson, G.R., (1996); *A new procedure for detecting nonlinearity from transient data using the Gabor transform*. Nonlinear Dynamics, 11(3), pp. 235-254.

[68] Staszewski, W.J., (2000); *Analysis of nonlinear systems using Wavelets*. Proceedings of the Institution of Mechanical Engineers, Part C, Journal of Mechanical Engineering Science, 214, pp. 1339-1353.

[69] Newland, D.E., (1999); *Harmonic Wavelets in Vibrations and Acoustics*. Philosophical Transactions: Mathematical, Physical and Engineering Sciences, 357(1760), pp. 2607-2625.

[70] Erlicher, S., Argoul, P., (2007); *Modal identification of linear non-proportionally damped systems by Wavelet transform*. Mechanical Systems and Signal Processing, 21(3), pp. 1386-1421.

[71] Feldman, M., Braun, S., (1994); *Identification of Non-linear systems parameters via the instantaneous frequency: application of the Hilbert transform and Wigner-Ville techniques*. Proceedings of the 13th International Modal Analysis Conference, p. 637.

[72] Bonato, P., Ceravolo, R., De Stefano, A., (1997); *Time-Frequency and ambiguity function approaches in structural identification*. ASCE Journal of Engineering Mechanics, 123(12), pp. 1260-1267.

[73] Wang, L., Zhang, J., Wang, C., Hu, S., (2003); *Time-frequency analysis of nonlinear systems: the skeleton linear model and the skeleton curves*. Transactions of the ASME, Journal of Vibration and Acoustics, 125, pp. 170-177.

[74] Wu, M., Smyth, A.W., (2008); *Real-time parameter estimation for degrading and pinching hysteretic models*. International Journal of Non-Linear Mechanics, 43, pp. 822-833.

[75] Carmona, R., Hwang, W.L., Torrésani, B.P., (1998); *Practical Time-Frequency Analysis*, San Diego, CA 92101-4495, USA Academic Press.

[76] Yang, J.N., Lin, S., (2004); *On-line identification of non-linear hysteretic structures using an adaptive tracking technique*. International Journal of Non-Linear Mechanics, 39, pp. 1481-1491.

[77] Shinozuka, M., Yun, C., Imai, H., (1982); *Identification of linear structural dynamic systems*. ASCE Journal of Engineering Mechanics, 108(6), pp. 1371-1390.

[78] Yang, J.N., Lin, S., Huang, H., Zhou, L., (2006); *An adaptive extended Kalman filter for structural damage identification*. Structural Control and Health Monitoring, 13(4), pp. 849-867.

[79] Zhang, H., Foliente, G.C., Yang, Y., Ma, F., (2002); *Parameter identification of inelastic structures under dynamic loads*. Earthquake Engineering & Structural Dynamics, 31(5), pp. 1113-1130.

[80] Shinozuka, M., Ghanem, R., (1995); *Structural system identification II: Experimental verification*. ASCE Journal of Engineering Mechanics, 121(2), pp. 265-273.

[81] Smyth, A.W., Masri, S.F., Chassiakos, A.G., Caughey, T.K., (1999); *On-line parametric identification of MDOF nonlinear hysteretic systems*. ASCE Journal of Engineering Mechanics, 125(2), pp. 133-142.

[82] Hernandez-Garcia, M.R., Masri, S.F., Ghanem, R., Figueiredo, E., Farrar, C.R., (2010); *An experimental investigation of change detection in uncertain chain-like systems*. Journal of Sound and Vibration, 329, pp. 2395-2409.

[83] Sato, T., Qi, K., (1998); *Adaptive H∞ filter: its application to structural identification*. ASCE Journal of Engineering Mechanics, 124(11), pp. 1233-1240.

[84] Li, S.J., Suzuki, Y., Noori, M., (2004); *Identification of hysteretic systems with slip using bootstrap filter*. Mechanical Systems and Signal Processing, 18(4), pp. 781-795.

[85] Li, S.J., Suzuki, Y., Noori, M., (2004); *Improvement of parameter estimation for non-linear hysteretic systems with slip by a fast bayesian bootstrap filter*. International Journal of Non-Linear Mechanics, 39(9), pp. 1435-1445.

[86] Li, S.J., Yu, H., Suzuki, Y., (2004); *Identification of non-linear hysteretic systems with slip*. Computers and Structures, 82, pp. 157-165.

[87] Andrieu, C., Doucet, A., Tadic, V.B., (2005); *Online simulation-based methods for parameter estimation in non-linear non-Gaussian state-space models*. Proceedings of 44th IEEE Conference on Decision and Control and European Control Conference EEC, Seville.

[88] Spiridonakos, M.D., Poulimenos, A.G., Fassois, S.D., (2010); *Output-only identification and dynamic analysis of time-varying mechanical structures under random excitation: A comparative assessment of parametric methods*. Journal of Sound and Vibration, 329, pp. 768-785.

[89] Poulimenos, A.G., Fassois, S.D., (2006); *Parametric time-domain methods for non-stationary random vibration modelling and analysis - A critical survey and comparison*. Mechanical Systems and Signal Processing, 20, pp. 763-816.

[90] Xiuli, D., Fengquan, W., (2010); *Modal identification based on Gaussian continuous time autoregressive moving average model*. Journal of Sound and Vibration, 329, pp. 4294-4312.

[91] Xie, Z., Feng, J., (2011); *Real-time nonlinear structural system identification via iterated unscented Kalman filter*. Mechanical Systems and Signal Processing, doi: 10.1016/j.ymssp.2011.02.005.

[92] Feldman, M., (1994); *Non-linear system vibration analysis using Hilbert transform - I. Free vibration analysis method 'Freevib'*. Mechanical Systems and Signal

Processing, 8(2), pp. 119-127.

[93] Feldman, M., (1994); *Non-linear system vibration analysis using Hilbert transform - II. Forced Vibration analysis method 'Forcevib'*. Mechanical Systems and Signal Processing, 8(3), pp. 309-318.

[94] Carson, J.R., (1922); *Notes on the Theory of Modulation*. Proceedings of the Institute of Radio Engineers, pp. 57-64.

[95] Cohen, L., (1995); *Time-Frequency Analysis*, Englewood Cliffs, NJ Prentice-Hall Inc.

[96] Feldman. (1999) References on the Hilbert Transform Applications and Non-Linear Vibration. [Online]. http://www.hitech.technion.ac.il/~feldman/hilbert.html

[97] Petrangeli, M.P., Spina, D., Valente, C., (1992); *The Non-linear Hilbert Transform Technique for the Identification of Dynamic Behaviour of Bridge Decks*. ISMES Identificazione strutturale: metodi dinamici e diagnostica, Bergamo.

[98] De Stefano, A..S.D., (1997); *The Use of Hilbert Transform and Neural Intelligence in Structural Non-Linearity Detection*. Journal of Structural Control, 1, pp. 89-105.

[99] Ceravolo, R., Demarie, G.V., Erlicher, S., (2010); *Instantaneous identification of degrading hysteretic oscillators under earthquake excitation*. Structural Health Monitoring, 9(5), pp. 447-464.

[100] Argoul, P., Ceravolo, R., Demarie, G.V., Sabia, D., (2010); *Instantaneous identification of localized non-linearities in steel framed structures*. Mécanique & Industries, 11, pp. 105-116.

[101] Demarie, G.V., Ceravolo, R., Sabia, D., Argoul, P., (2011); *Experimental Identification of beams with localized nonlinearities*. Journal of Vibration and Control, 17(11), pp. 1721-1732.

[102] Ceravolo, R., (2004); *Use of instantaneous estimators for the evaluation of structural damping*. Journal of Sound and Vibration, 274, pp. 385-401.

[103] Torczon, V., (1997); *On the convergence of patter search algorithms*. SIAM Journal on Optimization, 7(1), pp. 1-25.

[104] Bouc, R., (1971); *Modèle mathématique d'hystérésis (Mathematical Model of Hysteresis)*. Acustica, 24, pp. 16-25.

[105] Baber, T.T., Wen, Y.K., (1981); *Random vibrations on hysteretic, degrading systems*. ASCE Journal of Engineering Mechanics, 107(6), pp. 1069-1087.

[106] Wen, Y.K., (1976); *Method of random vibration of hysteretic systems*. ASCE Journal of Engineering Mechanics, 102, pp. 249-263.

[107] Erlicher, S., Point, N., (2004); *Thermodynamic admissibility of Bouc-Wen-type hysteresis models*. Comptes Rendus Mécanique, 332(1).

[108] Erlicher, S., Point, N., (2006); *Endochronic theory, non-linear kinematic hardening rule and generalized plasticity: a new interpretation based on a generalized normality assumption*. International Journal of Solids and Structures, 43(14-15), pp. 4175-4200.

[109] Erlicher, S., Bursi, O.S., (2007); *Bouc-Wen-type models with stiffness degradation: thermodynamic analysis and applications*. ASCE Journal of Engineering Mechanics.

[110] Simmons, G.F., (1966); *Introduction to Topology and Modern Analysis*, McGraw-Hill Inc.

[111] Charalampakis, A.E., Koumousis, V.K., (2008); *Identification of Bouc-Wen hysteretic systems by a hybrid evolutionary algorithm*. Journal of Sound and Vibration, 314, pp. 571-585.

[112] Sireteanu, T., Giuclea, M., Mitu, A.M., (2010); *Identification of an extended Bouc-Wen model with application to seismic protection through hysteretic devices*. Computational Mechanics, 45, pp. 431-441.

[113] Ikhouane, F., Mañosa, V., Rodellar, J., (2007); *Dynamic properties of the hysteretic Bouc-Wen model*. Systems & Control Letters, 56, pp. 197-205.

[114] Kalman, R.E., (1960); *A New Approach to Linear Filtering and Prediction Problems*. ASME Journal of Basic Engineering, 82, pp. 35-45.

[115] Jazwinski, A.H., (1966); *Filtering for nonlinear dynamical systems*. IEEE Transactions on Automatic Control, 11(4), pp. 765-766.

[116] Stengel, R.F., (1994); *Optimal Control and Estimation*, Dover.

[117] Julier, S.J., Uhlmann, J.K., Durrant-Whyte, H.F., (1995); *New approach for filtering nonlinear systems*. Proc. Am. Control Conference, pp. 1628-1632.

[118] Julier, S.F., Uhlmann, J.K., Durrant-Whyte, H.F., (2000); *A new method for the nonlinear transformation of means and covariances in filters and estimators*. IEEE Trans. Automat. Control, 45(3), pp. 477-482.

[119] Sarkka, S., (2004); *Recursive Bayesian Inference on Stochastic Differential Equations*. Helsinki University of Technology, PhD Thesis.

[120] Wan, E.A., Van der Merwe, R., (2001); *Kalman filtering and Neural Networks*, Wiley.

[121] Gong, X., (2004); *The study of challenge technology of single observer passive location and tracking using frequency rate and differential direction of arrival*. National University of Defense Technology, Changsha PhD Thesis.

[122] Kerschen, G., Peeters, M., Golinval, J.C., Vakakis, A.F., (2009); *Nonlinear normal modes, Part I: A useful framework for the structural dynamicist*. Mechanical Systems and Signal Processing, 23, pp. 170-194.

[123] Peeters, M., Viguié, R., Sérandour, G., Kerschen, G., Golinval, J.-C., (2009); *Nonlinear normal modes, Part II: Toward a practical computation using numerical continuation techniques*. Mechanical Systems and Signal Processing, 23, pp. 195-216.

[124] Smyth, A.W., Masri, S.F., Kosmatopoulos, E., Chassiakos, A.G., Caughey, T.K., (2002); *Development of adaptive modelling techniques for non-linear hysteretic systems*. Int. J. of Non-Linear Mech., 37, pp. 1435-1451.

[125] Pei, J.S., Smyth, A.W., Kosmatopoulos, E., (2004); *Analysis and modification of Volterra/Wiener networks for the adaptive identification of non-linear hysteretic dynamic systems*. J. of Sound and Vib., 275, pp. 693-718.

[126] Walczak, S., Cerpa, N., (1999); *Heuristic principles for the design of artificial neural networks*. Information and Software Technology, 41, pp. 107-117.

[127] Argoul, P., Le, T.-P., (2003); *Instantaneous indicators of structural behaviour based on the continuous cauchy wavelet analysis*. Mechanical Systems and Signal Processing, 17(1), pp. 243-250.

[128] Fan, Y., Li, C.J., (2002); *Non-linear system identification using lumped parameter models with embedded feedforward neural networks*. Mechanical Systems and Signal Processing, 16, pp. 357-372.